Measuring and Pricing Physical Climate Risk

Yannis Yuan [a]

[a] National University of Singapore

November 2025

Abstract

This paper develops a ground-up measure of firm-level physical climate risk by mapping forward-looking climate hazard projections to firms' geographically distributed asset holdings. The climate exposure factor (CEF) captures the expected fractional loss in physical asset value from future climate disasters, derived from hazard distribution and damage functions. Using this measure, we document a sizable and robust climate exposure premium of 5.82% per annum in a long-short portfolio, which remains significant after controlling for standard risk factors and firm characteristics. We provide primary evidence that *ex ante* physical climate risk is priced in the equity market through a preference-driven channel. As physical risk realizes through disasters, high-exposure firms experience persistent declines in operating profitability that are eventually reflected in prices.

Keywords: Climate Change, Physical Risk, Stock Returns, Sustainable Investing

JEL Classification: G12, G14, Q54

I. Introduction

The assessment of economic impacts of climate change has been significantly advanced by the development of integrated assessment models, where corporate carbon emissions and the resulting climate damages are incorporated into the dynamics of climate-economy system. Pioneered by Nordhaus (1991), these models scientifically evaluate the environmental externalities of economic activities using a shadow price, the "social cost of carbon," which reflects the trade-off between immediate consumption and long-term welfare. In comparison, measuring climate impact at the firm level remains challenging, as it requires careful attribution of climate damages to firms based on their exposure rates. Existing measures derived from news sentiment, ESG ratings, and corporate disclosures capture perceived climate risk but lack grounding in physical science models of actual financial losses due to climate change. This disconnect between perception and projected physical climate outcomes obscures the fundamental economic consequences of climate exposure.

In this paper, we propose a ground-up approach to measure the firm-level physical climate risk by mapping projected climate hazards to firms' physical asset holdings across geographical locations with varying loss distributions. As the climate crisis manifests in increasingly frequent and severe disasters, the likelihood that these events cause physical damages to firms' assets rises substantially. We estimate the aggregate climate exposure for the firm as the total expected loss of its physical asset value due to these climate disasters. A major advantage of this approach is that it leverages the forward-looking climate outcomes simulated using climate models under different socioeconomic scenarios to generate a science-based firm-level climate impact measure – a more scalable and objective approach than ESG ratings and text-based method like Sautner et al. (2023).

To systematically describe how physical risk affects firms' asset value, we propose a stochastic model that incorporates stylized features of climate hazards into asset dynamics. Specifically, we make adaptations to Merton (1974) model by introducing a Poisson jump process to capture the abrupt asset value changes caused by acute climate disasters. The jump-diffusion

structure has gained popularity in macro-finance over the years to explain the "equity premium puzzle" of Mehra and Prescott (1985). In these settings, rare macroeconomic disasters can cause drastic declines in aggregate consumption, as characterized by jumps in consumption growth, for which investors demand a higher equity premium (Barro, 2006, 2009; Barro and Jin, 2011; Gabaix, 2012). We depart from these consumption-based models, directly connecting climate disaster risk to financial losses by calibrating stylized damage functions for different climate disasters such as coastal and riverine floods. Specifically, the expected loss from physical risk can be attributed to three major determinants, namely *hazard*, *exposure* and *vulnerability* (IPCC, 2012). In this paper, we model them as three independent factors, where the exposure is solely determined by a firm's asset holdings in the region and the vulnerability depends on the climate resilience of these physical assets. The hazard factor is assumed to be completely exogenous to the firm's operations, described by the Poisson jump in terms of damage size and frequency.

Our ground-up climate assessment strategy can be implemented in a pipeline of four steps. First, we calibrate damage functions based on empirical studies of historical climate events. Among common concave functional forms used for asset-level climate hazard modeling, we select an exponential damage function that effectively maps the intensity of a climate event to fractional losses in asset value. The exponential structure achieves both excellent empirical fit and exceptional model simplicity that delivers superior interpretability in our valuation paradigm. Second, we estimate the probability distribution of asset damage sizes using forward-looking climate scenarios. These climate scenarios, presented in gridded heatmaps, provide science-based climate hazard intensity forecasts given different carbon transition pathways. Moreover, the return levels of hazard intensities provided by these scenarios allow us to accurately model the probabilities of extreme events. Third, we fit the extreme value distribution of climate damages to a hybrid normal-exponential distribution. The hybrid distribution has a well-defined moment generating function that produces analytically tractable loss projections at a future time under any given climate

scenario. And fourth, we map these climate-exposed assets through ownership to firms to derive a corporate climate exposure factor that reflects firms' total expected loss from physical disasters.

Our results reveal a clear division between climate-exposed and climate-insulated assets. Only 11.9% of more than 1.2 million physical assets are exposed to flood risk, whereas 88.1% remain insulated from climate disasters across all carbon transition scenarios. In particular, riverine flood risk is more pervasive in the United States, affecting about twenty times as many assets as coastal flooding. Coastal floods, on the other hand, are more severe on average, with a mere 84.6% expected retention rate (i.e., one minus damage rate), compared to 96.9% per year for riverine floods. Over time, expected damages from these climate events are projected to intensify, with the retention rate from coastal floods projected to decline from 87.8% in 2030 to 80.6% in 2080. For a physical asset exposed to coastal flooding in 2030, this retention rate translates into a cumulative loss of about half its value over a five-year horizon. Even under a coordinated decarbonization pathway, US physical risk damages remain largely unchanged, unfortunately, because emissions mitigation does not meaningfully reduce the highly uneven, location-specific impacts. As a result, firms with substantial assets in exposed regions continue to face escalating physical losses.

We apply this approach and quantify physical climate exposure for 4,349 firms. The intensity measure, climate exposure factor (CEF), is constructed by aggregating the asset-level expected climate damages over a 30-year useful life, normalized by each firm's total physical asset holdings. It represents a firm's expected fractional losses in total physical asset value from climate disasters. Firms in Biotechnology, Electric Utilities, and Energy Equipment & Services have the highest average exposure at 9.5%, 9.0%, and 8.1% of their total physical asset value respectively, compared to the sample mean at 4.6%. We show that our climate exposure measure is nearly orthogonal to alternative climate risk proxies, such as carbon intensity, firm climate sensitivity scores, or the text-based firm-disclosed climate risk measures of Sautner et al. (2023). This distinction underscores our effort to provide a structural and scalable framework for firm-level climate risk assessment that remains independent of expert, managerial, investor, or public perceptions.

Using our proposed intensity measure, we run a battery of tests to study the empirical relation between firms' physical climate exposure and expected stock returns. We first assign firms to quintile portfolios over the sample period from September 2003 to March 2024 by sorting on the climate exposure factor (CEF). We document an economically and statistically significant climate exposure premium of 5.82% per annum from a portfolio that simultaneously takes a long position in the top CEF quintile (median CEF = 7%) and a short position in the bottom quintile (median CEF = 0). This return premium cannot be fully explained by common risk factors, including Fama and French (1993, 2015), Carhart (1997), and Hou, Xue, and Zhang (2015), as the portfolio alpha remains substantial at 4.94%–6.13% per annum. This positive relation between climate exposure and expected returns is confirmed by Fama-MacBeth regressions.

Standard theories of climate risk pricing offer two distinct mechanisms to explain a climate exposure premium. Under a *value*-based view, firms exposed to climate risk face greater fundamental uncertainties, which can translate into higher expected returns to compensate investors for bearing systematic risk. Barnett, Brock, and Hansen (2020) exemplify this mechanism by incorporating climate state variables into macroeconomic dynamics, showing how climate uncertainties affect the stochastic discount factor and influence asset prices. Relatedly, Bolton and Kacperczyk (2021, 2023) provide empirical evidence that carbon emissions raise firms' cost of capital, which induces an equity green premium. Darrien et al. (2025) further demonstrate that poor ESG performance affects future cash flows. Under a *preference*-based view, investors exhibit nonpecuniary demand for sustainability characteristics, which influences prices independently of fundamentals. If a subset of investors prefers climate-resilient firms, these assets become overvalued, implying lower expected returns despite similar risk. Pástor, Stambaugh, and Taylor (2021, 2022) formalize this mechanism: shifts in climate concern generate time-varying demand for green assets, creating valuation gaps not justified by fundamentals. Empirically, salient climate events can trigger temporary demand shocks, generating capital flows toward climate-insulated

firms and away from exposed firms. The resulting short-run return patterns are documented by Dessaint and Matray (2017), Choi, Gao, and Jiang (2020), and Alok, Kumar, and Wermers (2020).

To disentangle the two possible channels, we exploit the return dynamics surrounding thirty most severe flood disasters between 2000 and 2024. We document significant preference-driven capital flows triggered by climate salience. Following the methodology of Gibson Brandon, Krueger, and Mitali (2021), we track shifts in institutional climate aversion through changes in 13-F holdings. Post-disaster, capital systematically flows toward low-exposure "safe-haven" assets, generating short-run outperformance relative to high-exposure peers. This flight-to-safety premium is transient: it peaks within one month and fully reverses in the following month as the salience of climate events fades. Crucially, this pattern operates independently of realized climate damages – the premium emerges even among firms with no direct asset impairment, suggesting flows are driven by shifts in climate preference rather than immediate cash-flow shocks. We argue that this same preference-based mechanism drives the persistent, unconditional climate premium observed over longer horizons. In particular, institutional sustainability mandates and strategies create limits to arbitrage that constrain corrections of preference-driven mispricings.

Importantly, our finding that pricing is driven by preferences does not imply that the risk is financially irrelevant. On the contrary, we validate that our measure captures material corporate climate risk. We show that among firms directly affected by flood disasters, operating profitability declines significantly in proportion to our exposure intensity measure. This confirms that the measure successfully identifies firms facing real cash-flow vulnerabilities. However, the market fails to price this fundamental risk *ex ante*. We find that this profitability deterioration translates into price adjustments only with a six-month lag, coinciding with the release of quarterly financial statements. This delayed recognition implies a market inefficiency: investors price the *ex ante* climate exposure through a preference channel but fail to incorporate its fundamental implications until the damages are realized.

Our study contributes to the growing literature of climate and sustainable finance in two major aspects. First, we introduce a novel approach to physical climate risk measurement. This approach is the first in the finance literature to systematically link firms' asset ownership to projected hazard maps on a large scale. Prior work focuses extensively on the local exposure of firms' headquarters (Hong, Li, and Xu, 2019; Alok, Kumar, and Wermer, 2020), suppliers (Pankratz and Schiller, 2024), and housing properties (Bernstein, Gustafson, and Lewis, 2019; Baldauf, Garlappi, and Yannelis, 2020, Giglio et al, 2021). Some studies resort to indirect measures such as firm-reported (Sautner et al., 2024) and analyst-assessed materiality measures. Our measure isolates transition risk and provides an objective, forward-looking metric grounded in scientific hazard projections and granular asset-level data. Though centered around flood risk, one of the most eminent physical hazard types, our approach can be extended to other natural disasters like wildfire and storms.

Second, we contribute to the literature on corporate sustainability, firm value, and market returns from a physical risk perspective. Bolton and Kacperczyk (2021, 2023) provide global evidence for an equity premium among firms with higher carbon emissions, a key metric for transition risk. On the other hand, Pástor, Stambaugh, and Taylor (2021) document realized outperformance of green assets due to a portfolio tilt and capital inflows. This contrast is explained by the pricing of expected versus realized returns. We extend the discussion to physical risk. We document a persistent climate exposure premium in cross-section, beyond short-lived sentiment responses to salient climate events (Dessaint and Matray, 2017; Choi, Gao, and Jiang, 2020). We also reconcile this with evidence that sustainability enhances firm value (Edmans, 2011; Chava, 2014; Albuquerque, Koskinen, and Zhang, 2019) by showing that physical climate impacts materialize through sustained declines in long-term profitability.

The rest of this paper is organized as follows. Section II describes the data. Section III explains our methodology to construct the firm-level climate impact measure. Section IV presents the empirical results of climate impact on stock returns. Section V provides an economic

explanation of the observed climate exposure premium in cross-sectional stock returns. Section VI concludes the paper.

II. Data

A. Data on Physical Assets

We use physical asset data from S&P Trucost. The asset-level dataset contains geographical locations, asset type and ownership information for over 4.87 million assets spread across more than 200 countries and territories globally. In the United States, we observe more than 1.2 million unique assets owned by 20,083 firms identified by GVKEY as of now. These assets include company headquarters, office locations, retail shops, branches, properties, power plants and other industrial facilities. The dataset is prepared through S&P proprietary data collection and acquisitions of other data vendors specializing in different types of assets. This dataset is crucial for the empirical implementation of our firm-level climate impact assessment framework. While full coverage of all assets is virtually infeasible, the number of firms involved alongside the geographical distribution of these assets ensure satisfactory representation of the actual physical risk exposure of firms in the United States and the developed world in general. We map the asset addresses at county and state levels based on their longitudes and latitudes using geocoders. Figure 1 illustrates the numbers of assets located by US county.

B. Data on Firm Characteristics and Financials

We obtain firm financial data from 2003 to 2024 based on the global factors data prepared by Jensen, Kelly, and Pedersen (2023). These factors are constructed using the firm characteristics from CRSP and Compustat databases. We use JKP23 factors directly instead of raw characteristics for better consistency across firms and over time. From these factors, we extract firms' revenues, debt, market capitalization, physical assets and industry classification. In addition, we obtain stock returns from CRSP database. We rely on the GIC 6-digit industry code (unless otherwise specified) for our subsequent industry-wide analysis.

C. Data on Projected Climate Hazard Intensities

We use the hazard maps for future coastal flood and riverine flood intensities from WRI Aqueduct. These hazard maps measure the intensity of flood risk by inundation depth in meters. Aqueduct models river and coastal hazards by downscaling or re-scaling extreme value distributions of water discharge volumes from a wide range of established global climate models (GCMs) under different representative concentration pathway (RCP) conditions and substituting them into economic damage functions based on regional economic productions and demographics (Ward et al., 2020). We consider two contrasting climate scenarios, namely a business-as-usual (BAU) scenario proxied by IPCC RCP8.5 pathway, and an intermediate transition scenario proxied by IPCC RCP4.5 pathway. The former models a persistent growth in carbon emissions throughout the 21st century, while the latter assumes a peak of carbon emissions around 2045 and a decline to approximately half the amount by 2100 (IPCC, 2012). Inundation depths are provided in 30" × 30" gridded maps for 2, 5, 10, 25, 50, 100, 250, 500, and 1,000-year return periods in 2030, 2050 and 2080. These return periods represent different frequencies at which an extreme climate disaster occurs.

D. Data on Empirical Flood Damage Curves

We model direct flood damage to assets using the EU JRC global flood depth-damage database. The damage curves for the United States are constructed based on FEMA's HAZUS data and are differentiated among building types including commercial, residential, industrial, transport and infrastructure (Huizinga, De Moel, and Szewczyk, 2017). The dataset converts average dollar damages to normalized damage factors at discrete flood depths of 0, 0.5, 1, 1.5, 2, 3, 4, 5, and 6 meters. These damage factors represent the fractional economic losses of asset values after a flood of a certain return period occurs in the asset location and can proxy for hazard severity across regions in the world and over time. We fit these key damage points to a continuous and smooth function to handle any arbitrary inundation levels. Figure 2 illustrates the US flood damage

curves by building type from the JRC database fitted to exponential cumulative distribution functions.

D. Data on Macroeconomic Variables

We rely on Federal Reserve Economic Data (FRED) from Federal Reserve Bank of St. Louis for macroeconomic data. In particular, we use the consumer price index (CPI) to adjust inflation of financial values, and market volatility index (VIX) to measure market risk. We measure the default spread (DEF) by taking the difference between Baa and Aaa corporate bond yield from Moody's. We measure the term spread (TERM) by taking the difference between 10-year and 3-month Treasury yields. We measure consumer sentiment (CSENT) using the index from the University of Michigan. All variables are rescaled at monthly frequency.

E. Data on Public Attention to Climate Change

We use the media climate change concerns (MCCC) index developed by Ardia et al. (2023) to proxy the level of public attention to climate-related issues. The index creates the news media corpus based on climate-related articles from ten leading US newspapers including the *Wall Street Journal*, *Washington Post*, and *New York Times*. It is classified into about thirty climate change themes, among which this paper focuses on three specific topics – hurricanes/floods, climate legislations/regulations, and carbon reduction technologies – to represent public sentiment of physical risk, regulatory risk, and technology risk respectively. Compared to other popular climate change news indices such as Engle et al. (2020), this index delves into specific climate issues with a longer coverage period from January 2003 to the date this paper is written.

F. Data on Historical Flood Events

We rely on two US climate disaster accounts. The first one is the losses from natural disasters developed by the Federal Reserve Bank of New York. This dataset provides county-level monthly economic damages from flood events since 1996. We use this data source to identify firms that experience realized climate damages over the period, thereby differentiating firms' realized climate losses from price effects on expected climate risk. To obtain these historically flooded firms, we

first select all flood events with a minimum inflation-adjusted total economic damage of USD 10 million. These make up a list of over 1,500 unique flood counts. Next, we map Trucost physical assets to each county and label whether each of these assets is affected by each event on the list. We then set a minimum threshold of 15% of a firm's assets located in the county to qualify a flood count. This empirical threshold is chosen in consideration of observed climate effects on firms' future profitability discussed in IV.D. With these filters, we classify firms into those with unrealized climate impact (i.e., never affected by a single flood event) and those with realized climate impact.

The second data source is the Billion-Dollar Weather and Climate Disasters from the NOAA National Centers for Environmental Information (NCEI) for high-severity historical flood events in the United States. We select all flood events with an inflation-adjusted economic damage of above USD 1 billion occurring between 2000 and 2024. The list consists of thirty events, with year/month and affected regions provided in the description. We map the affected states reported in the description to each of these events and tabulate them in Table A10. Compared to the New York Fed data source, this shortlist of thirty events have a more pervasive impact, often affecting multiple states. Therefore, these events are more salient but less granular than the New York Fed account. We use these most severe flood disasters in our event study to test market reactions to physical climate risk for firms both with and without realized climate impact.

III. Constructing a Firm-Level Physical Climate Risk Measure

A. Calibration of Asset-Level Damage Functions

To measure firm-level climate impacts, we first quantify the expected losses due to climate disasters at the asset level. This process involves several climate risk modeling challenges: (1) mapping climate disaster intensities to economic damages, (2) modeling probability distribution of damages, and (3) forecasting climate conditions and the resulting climate damages. We address each of these challenges in this section. The first challenge is where damage functions can be helpful. They answer the question of "what is the magnitude of financial damage to my building

when the flood depth is at 2 meters." In our analysis of climate hazards, we assume a time-invariant concave function of hazard intensity (i.e., inundation depth for floods) bounded by [0, 1]. The time-invariance condition implies that no incremental climate adaptation such as waterproofing is implemented over time. The concavity suggests diminishing marginal damage, which is consistent with the historical records of flood damages recorded in the JRC database. Note that this property does not hold in general for macroeconomic modelling of climate damages, where a convex, upward-sloping damage curve is more popular (e.g., Coronese et al., 2019).

To ensure goodness of fit and preserve analytical tractability, we use the cumulative distribution function (CDF) of exponential distribution to fit the characteristic hazard intensities collected in the JRC database. The damage function is given as

$$h(x) = 1 - \exp(-\kappa x) \tag{1}$$

where κ is the exponential parameter that reflects asset *vulnerability* and varies with physical asset type. In general, a higher asset vulnerability corresponds to a steeper damage curve or fast-intensifying degrees of impairment with climate intensity. We calibrate the damage function by minimizing the sum of squared residuals with historical observations from the JRC database, weighted by their respective percentages of exposed assets in the US based on Trucost physical risk asset locations mapped to WRI Aqueduct flood hazard maps. This is to ensure the optimal empirical fit for our subsequent asset-level and firm-level analyses. Figure 2 provides a visual illustration of damage curves for different asset types, and Table A1 summarizes the calibrated vulnerability parameter and R^2 for each type of asset. Some other popular choices of natural hazard damage functions include sigmoid and hyperbolic tangent functions. Compared to these alternatives which also offer reasonable empirical fit, exponential CDF offers several desirable properties. First, the calibrated parameter κ can be directly interpreted as the time-invariant measure of asset vulnerability, independent of the climate system. Second, its functional form integrates naturally into the asset dynamics, allowing vulnerability to be represented in a tractable way. This point will be developed further in III.C.

Among all physical asset types, residential building has the highest vulnerability factor at 0.848, while commercial building has the lowest at 0.43. Transport, industrial building, infrastructure and agriculture sit in between these upper and lower bounds. The model fit with our exponential CDF damage function is satisfactory, and we achieve a R^2 higher than 0.98 for all physical asset types except residential building. This can be explained by the fact that residential building has a non-zero empirical damage factor when the flood depth is zero, whereas our model forces the damage curve to start at the origin to ensure a clear disaster signal such that zero hazard intensity strictly indicates non-occurrence.

B. Estimation of Climate Damage Probability Distribution

The WRI Aqueduct flood maps represent the distribution of hazard intensities using return levels, which indicate the severity of flood events expected to be exceeded at certain annual probabilities. For example, the "100-year return level" corresponds to a flood inundation level with a 1% chance of being exceeded in any year. Using these return levels, we estimate a Gumbel distribution by analyzing block maxima, or the peak flood events within each year. The Gumbel distribution is commonly applied in flood modeling and underpins the Aqueduct flood maps. This block maxima approach fixes the frequency of flood events at once per year and models the distribution of flood depth.

Let X be the climate hazard intensity measure (i.e., inundation depth for coastal and riverine floods), and the cumulative distribution function (CDF) of X can be expressed as

$$G(x; \mu_G, \beta_G) = \exp\left(-\exp\left(-\frac{x-\mu_G}{\beta_G}\right)\right) \tag{2}$$

where μ_G and β_G are location and scale parameters respectively for a Gumbel distribution. The CDF is invertible with an explicit expression for the distribution's quantile function, given by

$$Q(p; \mu_G, \beta_G) = \mu_G - \beta_G \ln(-\ln p) \tag{3}$$

where $0 < p < 1$. The two parameters can be estimated by minimizing the sum of squared residuals between estimated and observed return levels

$$\min_{\mu_G,\beta_G} \sum_i [x_i - \hat{x}_{p_i}(\mu_G, \beta_G)]^2 \tag{4}$$

subject to $\beta_G > 0$. This optimization can be implemented effectively using ordinary least squares (OLS) by pre-substituting p into the log odds term. We have 9 pairs of observations (T_i, x_i), where the return period $T_i \in \{2, 5, \dots, 1000\}$ is inversely correlated with annual probability $p_i = 1 - \frac{1}{T_i} \in \{0.5, 0.8, \dots, 0.999\}$. Understanding that our "observations" are also model-estimated outputs from climate scenarios, this calibration exercise effectively reverse-engineers the model parameters for subsequent integration into our financial model. For each unique geolocation l, we calibrate a unique hazard distribution $Gumbel(\mu_{G,l}, \beta_{G,l})$, where $\mu_{G,l}$ can be interpreted as the baseline hazard level and $\beta_{G,l}$ as the variability or tail thickness. They co-determine the local response to the climate system (e.g., topography, distance to the coast, elevation, drainage and land cover).

C. Modeling Asset Dynamics with Climate Impacts

Suppose a physical asset experiences a fractional loss h_t during a climate disaster

$$V_{t^+} = V_{t^-} \cdot (1 - h_t) = V_{t^-} \cdot e^{-J_t} \tag{5}$$

where we define the log damage rate $J_t = -\ln(1 - h_t) = \kappa x_t \geq 0$. We model the asset dynamics as a jump-diffusion process

$$d \ln V_t = \left(\mu - \frac{1}{2}\sigma^2\right) dt + \sigma dW_t - J_t dN_t \tag{6}$$

with a constant rate λ for the Poisson jump N_t. μ and σ are the constant drift rate and diffusion volatility in Merton (1974). In this setup, climate disaster is incorporated as an exogenous shock to the asset dynamics, introducing discontinuity to the random diffusion process. The jump rate λ is a measure of hazard *frequency* and is inherently set to 1 per year in our block maxima paradigm. Moreover, log damage rate J_t is explicitly expressed as a product of hazard intensity x_t and the

time-invariant asset vulnerability κ, thanks to our exponential CDF damage function. We can therefore derive a formula for the future value of asset

$$V_T = V_0 \exp\left(\left(\mu - \frac{1}{2}\sigma^2\right)T + \sigma W_T - \sum_{i=1}^{N_T} J_i\right) \tag{7}$$

where the three exponent terms represent constant drift, market risk, and climate risk respectively. We focus on parameterizing the jump term in this paper to evaluate asset exposure to climate physical risk, while the parsimonious model structure can be adapted to incorporate other factors such as carbon transition risk (e.g., in the diffusion drift and volatility) independent of the jumps. For $J_t \sim f_J$ with a well-defined moment generating function (MGF) $M_J(s)$, we can evaluate

$$E[V_T] = V_0 \exp\left(\mu T - \lambda T\big(1 - M_J(-1)\big)\right) \tag{8}$$

where $M_J(-1) = E[\exp(-J)]$.

We follow the procedure detailed in III.B to calibrate the probability distribution of flood intensities. Specifically, we estimate Gumbel-distributed annual flood depths in a block maxima approach. Given the linear relationship between log damage rate J_t and hazard intensity X_t, we have the log damage rate as a Gumbel random variable as well with $J_t \sim Gumbel(\kappa\mu_G, \kappa\beta_G)$, where μ_G and β_G are parameters of the original climate hazard intensity distribution. Unfortunately, Gumbel distribution does not have a tractable moment generating function (MGF). For computational ease, we need to re-parameterize the Gumbel-distributed log damages to ensure a closed-form expression for the future asset value. To account for the heavy tail of extreme events, we consider a hybrid distribution consisting of a normal core and an exponential right tail. With a cutoff right tail probability p, the density function of the normal-exponential hybrid distribution can be expressed as

$$f_J(j; \mu_N, \sigma_N^2, \eta) = \begin{cases} \dfrac{1-p}{\sigma_N}\dfrac{\phi((j-\mu_N)/\sigma_N)}{\Phi((J_p-\mu_N)/\sigma_N)}, & j \le J_p \\ p\eta\exp(-\eta(j-J_p)), & j > J_p \end{cases} \tag{9}$$

where $\phi(\cdot)$ and $\Phi(\cdot)$ are the PDF and CDF of standard normal distribution. We can integrate the probability densities of the two parts to show that the probabilities of the normal core and exponential tail are $1-p$ and p respectively. To ensure that the hybrid function is continuous at the cutoff point J_p, we have

$$\eta = \frac{1-p}{p\sigma_N} \cdot \frac{\phi((J_p - \mu_N)/\sigma_N)}{\Phi((J_p - \mu_N)/\sigma_N)} \tag{10}$$

Both normal and exponential distributions are common options for a jump-diffusion model to date due to their analytical tractability. Normal jumps are pioneered by Merton (1976) in credit risk analysis and remain the most popular setup in financial modelling. Exponential jumps are suggested by Kou (2002) in option pricing as an alternative to Black-Scholes model to address the leptokurtic (i.e., higher peak and heavier tails) feature of asset returns. Additionally, exponential-distributed log damages are equivalent to fractional losses that follow a power law distribution, which is commonly seen in consumption-based models like Barro and Jin (2011). In this paper, we emphasize the empirical fit as the primary reason besides tractability for selecting this normal-exponential hybrid structure. Parameters μ_N, σ_N^2 and η are calibrated using maximum likelihood estimation (MLE) with log damages simulated from the estimated Gumbel distributions. The implementation of the MLE is detailed in Appendix I. Figure 3 and Figure 4 illustrate the empirical fit of the normal-exponential hybrid distribution for coastal and riverine flood damages respectively. Tabel A2 summarizes the calibration results. We set $p = 0.3$ in this paper for the hybrid distribution as it can be shown using a grid search approach that this tail probability consistently offers desirable empirical fit. While the parameter can be optimized further in each individual calibration, there is little marginal gain in likelihood in doing so and we risk losing robustness across climate scenarios as a trade-off. Economically, the tail probability p marks the transition into the extreme territory, often seen in climate stress testing and tipping point analysis.

The corresponding quantile J_p is the minimum loss during a climate event at an extreme probability p, often regarded as the p climate value-at-risk (CVaR).

The MGF of the hybrid distribution is a combination of a normal MGF and an exponential MGF. To ensure that log damage J is defined over $(-\infty, +\infty)$, we manually introduce an indicator function that sets the MGF to 1 when $J \leq 0$. The MGF at $s = -1$ can now be expressed as

$$M_J(-1) = E\left[\exp(-J) \cdot \mathbf{1}_{\{J>0\}} + \mathbf{1}_{\{J\leq 0\}}\right]$$

$$= \begin{cases} 1 - \dfrac{p}{\eta+1}\exp(\eta J_p), & J_p \leq 0 \\ (1-p)\left[\Lambda_1 + \Lambda_2 \exp\left(-\mu_N + \dfrac{1}{2}\sigma_N^2\right)\right] + p\dfrac{\eta}{\eta+1}\exp(-J_p), & J_p > 0 \end{cases} \tag{11}$$

where $\Lambda_1 = \frac{\Phi\left(\frac{-\mu_N}{\sigma_N}\right)}{\Phi\left(\frac{J_p-\mu_N}{\sigma_N}\right)}$ and $\Lambda_2 = \frac{\Phi\left(\frac{J_p-\mu_N}{\sigma_N}+\sigma_N\right)-\Phi\left(\frac{-\mu_N}{\sigma_N}+\sigma_N\right)}{\Phi\left(\frac{J_p-\mu_N}{\sigma_N}\right)}$ are adjustments to the normal segment. With $\lambda = 1$, the measure M_J can be interpreted as the expected annual retention rate from climate disasters, and its complement $1 - M_J$ as the expected annual fractional loss rate. The flood maps from WRI Aqueduct allow us to estimate M_J for coastal and riverine floods in 2030, 2050, and 2080 using Eq. 11. We apply linear interpolation to the three estimates to fill for the years in between and calculate a time-weighted average annual retention rate $\overline{M}_J$ for a fifty-year period from 2030 to 2080. Recall from Eq. 8 that $E[V_T]/V_0 = \exp\left(\int_0^T (M_J(t) - 1)\lambda dt\right) = \exp\left(-\lambda T(1 - \overline{M}_J)\right)$. For example, if an industrial facility worth \$1 million today has an $M_J = 0.95$, the expected value of this facility next year net of interest rate and market volatility is $e^{-0.05} \approx$ \$0.95 million.

We perform this estimation pipeline for all Trucost assets located in the United States to estimate the annual retention rate for each asset under two climate scenarios: (1) a business-as-usual (BAU) scenario, modeled by IPCC RCP8.5; and (2) an intermediate transition scenario, modeled by IPCC RCP4.5. The results are summarized in Table 1. We make two key observations

about the asset-level climate exposures. First, a sizable fraction of physical assets are exposed to climate disasters under both scenarios. Of over 1.2 million assets in our sample, 143,164 (or 11.7%) are exposed to riverine flood under the BAU scenario, compared to 6,988 (or 0.6%) for coastal flood. If we assume an intermediate transition scenario where carbon emissions peak by around year 2045 and gradually decline afterwards, about 11.6% and 0.5% physical assets are exposed to riverine and coastal floods respectively, slightly below the numbers for the BAU scenario. These numbers largely stay unchanged over time, which suggest a clear geographical division between climate-exposed and climate-insulated regions. Across asset types, a greater fraction of agricultural assets are exposed to riverine floods. On the contrary, these agricultural assets are generally unaffected by coastal floods relative to other asset types. This cross-asset variation can be explained by the heterogenous asset concentrations in regions exposed to different types of climate disasters.

Second, exposed assets are subject to an average annual retention rate of 0.962 over the fifty-year period (under the BAU scenario, same hereafter unless otherwise specified), losing 3.7% of value every year on average. While riverine floods are more pervasive with a greater number of assets affected, coastal floods usually cause more severe damages to exposed assets. The expected annual retention rate from coastal floods is 0.846, compared to the retention rate from riverine floods at 0.969. Figure 5 plots the forward retention rates over time for coastal and riverine floods. Both kinds of flood disasters intensify over the 50-year period. This aligns with the scientific view that physical risk unfolds more gradually, and climate disasters will become more severe towards the end of the century (IPCC, 2022). The risk of coastal flooding experiences a more drastic escalation over time compared to riverine flooding, owing to the combined influences of sea level rise and extreme storms led by the rising temperature. Unfortunately, a low-carbon transition does not seem to substantially delay the heightened threat of extreme flooding in the US context. Figure 6 illustrates the cumulative retention factor over time under both climate scenarios. For both coastal and riverine floods, the retention curve under the intermediate transition scenario is hardly

differentiable from that under the BAU scenario. Many scholars suggest the divergent physical risk exposures around the world, which creates varying incentives for policymakers worldwide to make coordinated decarbonization efforts. In the US case, for example, Deschênes and Greenstone (2007) conjecture that random variation in temperature and precipitation due to climate change will benefit its agricultural sector.

D. Mapping Firm-Level Climate Exposures through Asset Ownership

Denote the average retention rate for asset w from climate disasters as $\overline{M}_w$, and we construct a measure to estimate the firm-level climate exposure value (CEV), expressed as

$$CEV_{i,t} = \sum_w V_{w,t}\left[1 - \exp\left(-\lambda T(1-\overline{M}_w)\right)\right] \tag{12}$$

where $V_{w,t}$ is the counterfactual (i.e., if there were no climate risk) asset value had there been no climate change impacts. Subscript t accounts for firm i's time-varying asset ownership. It represents the expected loss of physical asset value due to future climate disasters. $CEV_{i,t} = 0$ if none of firm i's assets are exposed to climate disasters. The measure is derived from Eq. 8 and we neglect the climate effects on discount rate to isolate our climate damage measure from other channels. To account for the size effect, we scale the absolute climate exposure measure by firms' total physical asset holdings and derive an intensity measure, climate exposure factor (CEF), given as

$$CEF_{i,t} = \frac{CEV_{i,t}}{\sum_w V_{w,t}} = \frac{\sum_w V_{w,t}\left[1 - \exp\left(-\lambda T(1-\overline{M}_{w,t})\right)\right]}{\sum_w V_{w,t}} \tag{13}$$

The measure represents the expected asset loss ratio due to climate change. The total physical asset $\sum_w V_{w,t}$ can be proxied by firm i's net property, plant and equipment (PP&E) at t. As a result, both $CEV_{i,t}$ and $CEF_{i,t}$ can be updated every quarter based on the firm's quarterly financial statements and physical asset holdings data. We may use Tobin's Q to estimate the market value of the firm's assets based on its book-to-market ratios.

In practice, however, firms' asset holding data is less accurate, less granular and updated less frequently compared to their financial data. We therefore need to make several assumptions during implementation. First, we assume firms' physical assets included in the Trucost dataset have equal financial values. We approximate a firm's $CEF_{i,t}$ by equally weighting its physical asset holdings. Second, we assume firms have not made substantial climate adaptation by selling or migrating its physical assets. In other words, there have not been asset ownership changes that cause a material shift in firms' climate exposure. After all, changes in firms' asset holdings are infrequent, evidenced by a relatively high lag-1 autocorrelation of PP&E series at 95%. However, we acknowledge that our measure discounts firms' climate adaptation efforts and is subject to asset look-ahead bias and firm survivorship bias. In IV.E, we implement some robustness tests to address these concerns.

We deploy these measures to publicly listed firms in the United States between June 1999 and March 2024, with at least one physical asset collected in the S&P Trucost physical risk dataset. We use JKP23 firm characteristics for consistent adjustments and merge them with the CRSP firm monthly return and price file. Our data sample includes a total of 4,349 firms and 746,416 firm-months. See Table A4 for a breakdown of these firms by industry. We rely on this sample for the majority of our empirical analysis.

Table 2 provides firm climate and financial summary statistics and cross-correlations. The climate variables include our CEF and CEV measures. The financial variables include market equity (ME), book-to-market ratio (B/M), return on equity (ROE), investment rate (I/A), tangible asset ratio (K/A), sales-to-asset ratio (S/A), and book leverage (Lev). We apply inflation adjustments to all monetary variables using the US consumer price index (CPI) and report all financial values in 2011 million USD unless otherwise noted. In Panel A, we report the pooled mean, standard deviation (Std. Dev.), 5th percentile (P5), 25th percentile (P25), median, 75th percentile (P75), 95th percentile (P95) together with total firm-month observations (N) for each of these climate and financial variables. The pooled average exposure factor is 0.04, which represents approximately 4% expected loss in physical asset value due to climate disasters over the next 30

years. In absolute terms, this pooled average exposure is at 63.53 million dollars (in 2011 USD). Firms in different industries exhibit distinct climate exposure statistics. Table A3 reports the top 10 industries by average climate exposure. Ranking by the intensity measure CEF, Biotechnology, Electric Utilities, and Energy Equipment & Services are the top three industries with an average expected fractional loss of 9.5%, 9.0% and 8.1% respectively. By the absolute book value measure CEV, Electric Utilities, Multi-Utilities, and Diversified Telecom Services are the top three industries.

In Table 2, Panel B, we present a correlation matrix among these climate and financial variables. CEF and CEV have a correlation of 0.17. The intensity measure is not strongly correlated with firm size, book-to-market ratio, profitability, investment rate, asset tangibility, sales-to-asset, and book leverage. The absolute measure, on the other hand, is significantly driven by firm size with a correlation of 0.58. It also correlates with asset tangibility measure (K/A) with a Pearson's correlation coefficient of 0.26.

We also investigate whether our firm-level climate exposure measures are correlated with other notable measures that have gained popularity in the climate finance community. Table A5 reports Pearson's correlation coefficients for our climate exposure measures with firms' greenhouse gas (GHG) emissions, S&P climate sensitivity scores, and frequencies of firm-reported climate-sensitive words in earnings conference calls compile by Sautner et al. (2023). GHG scope 1 and scope 2 measure the direct and indirect emissions of corporate activities and are often used to measure firms' climate transition risk (e.g., Pástor, Stambaugh, and Taylor, 2022; Bolton and Kacperczyk, 2023). S&P climate sensitivity scores, like the climate risk scores provided by other rating agencies, are popular among institutional investors with respect to portfolio climate risk mandates. Our intensity measure CEF is almost orthogonal to these alternative measures with nearly zero correlations. The absolute measure CEV positively correlates with absolute carbon emissions, mainly through the firm size channel. Its correlations with S&P climate sensitivity scores and firm-reported climate word counts are all below 15%. This suggests that our ground-

up approach, with its focus on physical risk drivers, potentially reveal new information about firms' exposure to climate change. In Section IV, we investigate the asset pricing implications of our climate exposure measures.

IV. Stock Market Reactions

A. Portfolio Sorting and Factor Regressions

We begin our empirical analysis by examining how firms' climate exposure relates to expected returns through a univariate portfolio sort. To isolate the effect of climate exposure from size-related distortions, we sort firms annually each March into value-weighted quintile portfolios based on the intensity-scaled climate exposure factor (CEF) described in Eq. 13. All characteristics used in the construction of CEF are lagged by at least one month to ensure that portfolio formation relies only on information available prior to the return-measurement period. Because our objective is to examine the pricing of *expected* rather than *realized* physical climate risk, we exclude firms that experience climate-related damages within the sample window from September 2003 to March 2024. Firms are classified as having unrealized climate risk according to the procedure outlined in II.F, and only these firms enter the CEF-sorted portfolios.

Table 3, Panel A reports the value-weighted excess returns for the CEF-sorted portfolios. We observe a pronounced monotonic relation between climate exposure and subsequent returns: the lowest-exposure quintile earns an annualized excess return of 5.21%, whereas the highest-exposure quintile earns 11.02%. This gradient suggests that firms more exposed to physical climate hazards command higher expected returns. To gauge the economic magnitude, we construct a long-short portfolio that buys the highest-exposure quintile (Q5) and sells the lowest-exposure quintile (Q1). The spread yields an annualized excess return of 5.82% with a *t*-statistic of 3.25, indicating that the climate exposure premium is both economically sizable and statistically precise. The monotonic increase across quintiles and the significant Q5–Q1 spread together provide preliminary evidence that physical climate risk is priced in the cross-section of stocks.

To assess whether the return differentials across the CEF-sorted portfolios are explained by known risk factors, we estimate time-series regressions of monthly excess returns for each quintile and for the Q5–Q1 spread on standard factor models. Panels B, C, and D of Table 3 report the estimated coefficients, alphas, *t*-statistics, and adjusted R^2. Panel B implements the FF3 model augmented with the Carhart (1997) momentum factor. Panel C uses the five-factor model of Fama and French (2015). Panel D applies the *q*-factor model of Hou, Xue, and Zhang (2015).

The factor regressions collectively show that the climate exposure premium is not subsumed by existing risk factors. Under the FF3+MOM specification, the Q5–Q1 spread delivers an annualized alpha of 6.13% ($t = 4.19$), indicating that the premium persists even after controlling for market, size, value, and momentum. The spread remains robust under both the FF5 model (5.17% per annum) and the HXZ *q*-factor model (4.94% per annum). Although the spread exhibits some exposure to size, profitability, and investment factors, these loadings are insufficient to explain the magnitude of the premium. Overall, the results confirms that the CEF-based return spread captures a distinct component of expected returns that is not spanned by standard factor structures.

Table 4 summarizes median firm characteristics across the CEF-sorted quintiles. The CEF measure rises from 0.00 in Q1 to 0.07 in Q5, with a large concentration of firms at or near zero exposure in the lower quintiles. When firms share identical CEF values, we break ties by ranking them according to the number of identified physical assets and assign firms with fewer assets to the lower portfolio. This refinement preserves strict univariate ordering and does not distort other portfolio characteristics. As expected, CEV co-varies with CEF across portfolios, consistent with their correlation shown in Table 2. Median log ME and ROE also increase across the quintiles, whereas B/M declines. Characteristics such as I/A, K/A, beta, and sales and capital growth ($\Delta S/S$, $\Delta K/A$) show no meaningful variation. To ensure that the observed climate effect is not driven by firm characteristics that vary across CEF quintiles, we perform bivariate portfolio sorting on size, value, and profitability (see Table A6). The stock return premiums remain robust.

B. Fama-MacBeth Regressions

To complement the portfolio evidence, we perform Fama-MacBeth regressions to examine whether CEF captures a distinct cross-sectional return premium after controlling for observable firm characteristics. Each month from September 2003 to March 2024, we regress annualized excess returns on CEF and the firm characteristics reported in Tables 2 and 4. Table 5 reports the time-series averages of the coefficients, *t*-statistics, and adjusted R^2. Across specifications, the CEF coefficient remains positive and highly significant, with *t*-statistics of 4.05–4.31 when including industry fixed effects (Columns 2 and 4). The results indicate that, even after accounting for size, value, profitability, and industry, firms with higher climate exposure earn systematically higher expected returns.

Figure 7 illustrates this relation visually: returns are benchmarked to the average of firms with zero climate exposure (Q1). For the portfolio-based estimates, we apply a smoothed quadratic spline to the quintile returns, yielding a continuous curve that reaches roughly 6% per annum at CEF ≈ 0.07 (Q5) for equally weighted portfolios, and just under 6% for value-weighted portfolios. The Fama-MacBeth estimates, which average across all firms each month, imply a somewhat milder curvature and a lower return premium of about 3.5% per annum at the same CEF level. Despite these differences in magnitude due to methodological aggregation, both approaches reveal a clear, monotonic positive relation between climate exposure and expected returns, providing strong and complementary evidence that firms with greater physical climate risk earn higher *ex ante* returns.

We use the term "climate exposure premium" throughout this paper to describe the return premium related to CEF. We do not claim this return spread as a systematic risk premium because (a) there is no evidence of climate risk as a standalone risk factor, and (b) the short history of possible manifestation of climate effects cannot substantiate such an argument. While the CEF measure we propose is constructed to represent firms' expected annual losses in physical asset value to capture their long-run climate risk, the realization of climate risk impacts typically relies

on common financial transmission channels, affecting firm value through changes in their cash flows or discount rates (Cornell and Damodaran, 2020). At the same time, a nonpecuniary preference for climate exposure can influence short-term stock performance also, as well documented in the corporate sustainability literature (e.g., Hong and Kacperczyk, 2009). The rest of the paper attempts to identify the pricing channels that explain the empirical climate premium.

C. Time-Series of Climate Exposure Premium

A key question for understanding the nature of climate exposure premium is whether it reflects fundamental risks or sentiment-driven fluctuations. Sentiment-driven factors typically display high short-term volatility and sharp reversals following exogenous shocks, whereas fundamental risk factors correspond to macroeconomic or structural changes and exhibit more persistent patterns. To distinguish these channels, we examine the time-series variation of a climate exposure factor-mimicking portfolio.

We construct the exposed-minus-insulated (EMI) portfolio following the Fama-French convention. Firms are ranked by CEF, and a value-weighted long position is taken in the top 1/3 of firms, while a short position is taken in the bottom 1/3. This ensures that EMI captures broad exposure to physical climate risk rather than extreme-tail dynamics. Figure 8 plots annualized EMI returns from September 2003 to March 2024, smoothed with a 12-month rolling mean. Returns remain predominantly positive, interrupted only by a few sharp, short-lived drawdowns, which likely reflect transient spikes in climate sentiment rather than fundamental shifts in firms' physical risk profiles.

To identify the drivers of these fluctuations, we regress EMI returns on climate salience indices and macroeconomic controls. Climate salience is measured by climate news indices (CNI) based on media climate change concerns compiled by Ardia et al. (2023). These indices capture public attention to global warming (physical risk), climate policy actions (regulatory risk), and carbon-reduction technologies (technological risk). Macroeconomic controls include the corporate-government bond default spread (DEF), the Treasury term spread (TERM), the

University of Michigan consumer sentiment index (CSENT), and the VIX. First differences are taken for CNI, VIX, and CSENT to address time-series nonstationarity, and all variables are aligned at month-end. Table 6 reports these regression results.

The evidence indicates that EMI returns respond systematically to climate news. During periods of heightened global warming coverage, EMI returns decline as high-exposure firms underperform relative to low-exposure firms (Column 1), reflecting temporary surges in investor preference for climate-insulated assets. Policy and technology news have weaker contemporaneous effects (Columns 2 and 3), which validates that our CEF-based portfolio primarily captures financially material physical climate risk rather than regulatory or technological risks. Despite these short-term fluctuations, the regression alpha remains positive and significant, confirming the long-run climate premium documented in IV.A–B.

Predictive regressions using one-month lagged variables (Columns 4–6) further reveal mean-reversion: the coefficients on climate news shocks reverse signs, indicating rapid correction in equity markets compared to real assets (Giglio et al., 2021) likely due to higher liquidity. Overall, these results suggest that short-term swings in physical, regulatory, and technological climate sentiment temporarily modulate realized returns, but the underlying long-term premium remains tied to firms' physical climate exposure.

D. Event Study

While the time series analysis in IV.C highlights the role of climate salience in the pricing of physical climate risk, it cannot establish whether observed return patterns reflect adjustments to fundamental risk or shifts in investor preference. When climate-exposed firms underperform during periods of high climate salience, this correlation could arise from (a) rational expectations about deteriorating future cash flows or discount rates (H1), or (b) preference-driven demand shifts unrelated to firm fundamentals (H2). Because climate news tends to convey information about broad climate risks rather than firm-specific changes in expected cash flows, the time-series evidence alone cannot separate these channels.

To isolate these mechanisms, we implement an event study exploiting the thirty most severe US flood events between 2000 and 2024 (inflation-adjusted economic damages ≥ USD 1 billion; see Table A10). We construct a disaster indicator, $Disaster_t$, equal to one in the month of an event; and a firm-specific indicator, $Affected_{i,t}$, equal to one if over half of a firm's physical assets are located in the disaster-affected states. Critically, we partition firms into two groups. The *unrealized* group – our primary sample in IV.A–C – has never experience a climate-related disaster in the sample window, so $Affected_{i,t} = 1$ captures proximity but not realized damages. The *realized* group – our control sample – has been directly hit at least once, so $Affected_{i,t} = 1$ is more likely to coincide with actual physical damages. This separation allows us to distinguish preference-driven return effects (which should occur for unrealized firms) from changes driven by genuine cash flow deterioration (which should arise only for realized firms).

We estimate the following regression

$$R_{i,t+\tau} - R_f = a + b_1 \times CEF_i + b_2 \times Disaster_t + b_3 \times CEF_i \times Disaster_t + b_4 \times CEF_i \times Disaster_t \times Affected_{i,t} + c \times Controls + \varepsilon_{i,t} \quad (14)$$

with standard controls in Table 2. Under the *value* hypothesis (H1), returns should respond meaningfully to disasters only when firms suffer actual impairments, which imply a negative and significant b_4. Under the *preference* hypothesis (H2), disasters trigger shifts in investor demand toward climate-insulated assets, so b_3 is expected to be negative and largely unrelated to whether firms are truly damaged.

Table 7, Panel A reports the return regression results. For unrealized firms, b_1 is positive, consistent with the unconditional climate exposure premium in IV.B. The CEF × Disaster term turns sharply negative one month after an event (t = –5.30) (Column 2), and this effect fully reverses in the following month (t = 6.90) (Column 3). This transient discount-and-rebound pattern is inconsistent with a value-based channel, since the disaster does not alter future physical risk, but aligns with preference-driven selling during salient events. The triple interaction is largely

muted, confirming that these firms do not experience actual damages. For realized firms, by contrast, the triple interaction becomes significant at a six-month horizon (Column 6), consistent with gradual operational disruptions and asset impairments that affect fundamentals rather than pricing of expected climate risk.

Table 7, Panel B examines investor preference shifts. Following Gibson Brandon, Krueger, and Mitali (2021), we construct a firm-specific investor climate aversion (ICA) measure based on institutional holdings from quarterly 13-F filings and analyze its quarterly change, ΔICA. Increases in ΔICA correspond to divestment from high-exposure firms and reallocation toward low-exposure firms. Because ΔICA reflects the rebalancing of climate-averse versus climate-tolerant investors it is designed to capture preference dynamics.

We estimate the following regression

$$\Delta ICA_{i,t+\tau} = a + b_1 \times CEF_i + b_2 \times Disaster_t + b_3 \times CEF_i \times Disaster_t + b_4 \times CEF_i \times Disaster_t \times Affected_{i,t} + c \times Controls + \varepsilon_{i,t} \quad (15)$$

The results show a sharp rise in ΔICA immediately after a disaster for unrealized firms (t = 15.06), reflecting broad divestment from high-exposure stocks (Column 1). The negative CEF × Disaster coefficient (t = –3.81) indicates that this rebalancing alters the composition of shareholder bases: high-exposure firms increasingly end up held by climate-tolerant investors, while low-exposure firms attract more climate-averse owners. This shift in ownership structure provides direct evidence of climate preference reallocation during salient events.

Table 7, Panel C evaluates long-run value impacts using profitability regressions

$$ROA_{i,t+\tau} = a + b_1 \times CEF_i + b_2 \times Disaster_t + b_3 \times CEF_i \times Disaster_t + b_4 \times CEF_i \times Disaster_t \times Affected_{i,t} + c \times Controls + \varepsilon_{i,t} \quad (16)$$

As expected, the triple interaction is strong negative for realized firms (t = –10.22), reflecting genuine deterioration in operating profitability after physical damage. No such effect appears for

unrealized firms (Column 5), confirming that their event window return swings do not map into changes in firm fundamentals.

Overall, the event study indicates that the *ex ante* climate exposure premium primarily reflects investor preference (H2): climate events generate short-lived return reactions and capital reallocation unrelated to firms' fundamental prospects. Value adjustments (H1) emerge only when firms incur actual climate damages, and these adjustments pertain to realized losses rather than the pricing of expected climate risk.

E. Robustness

E.1. Additional Empirical Tests

One strand of testing focuses on the robustness of alternative asset pricing explanations for observed climate-related market effects. On one hand, a persistent climate premium, if driven by investor preferences or market frictions, could represent a long-term asset mispricing that persists due to limits to arbitrage. Conversely, if the climate effect aligns with a value-based interpretation, it would be expected to manifest through changes in underlying corporate fundamentals, being subsumed by standard asset pricing factors and reflecting true economic value shifts rather than a market inefficiency.

Characteristics matching. In addition to the factor regressions in IV.A and Fama-MacBeth regressions in IV.B, we perform a pairwise characteristics matching for firms with similar market beta, size (log ME), value (log B/M), profitability (ROE), investment (I/A), asset tangibility (K/A), and sales-to-asset ratio (S/A) but differ in climate exposure (CEF). The results are summarized in Table A8. The return spread remains significant at the 99% confidence level after matching the six financial characteristics.

Limits to arbitrage. We test whether the persistence of the preference-induced climate effect on can be attributed to firms' idiosyncratic volatility, which creates a barrier to arbitrage. We use monthly idiosyncratic volatility after Fama-French three factors from the JKP23 dataset as a proxy. Specifically, we re-estimate the Fama-MacBeth regressions in IV.B by including IVOL and its

interaction with climate exposure, CEF × IVOL, to test whether the climate effect remains significant. The coefficient on the interaction term is positive and statistically significant, whereas CEF alone becomes insignificant. This indicates that the climate exposure premium is not uniform across firms; it is pronounced only where idiosyncratic risk is high and arbitrage is more constrained. Hence, the pricing impact of climate preference persists primarily when arbitrage is costly or risky, preventing full adjustment.

E.2. Data and Measurement Quality

Another strand of testing is around data and measurement quality. Our data sample includes all firms with at least one physical asset recorded in the S&P Trucost database. We manage to match 4,349 firms in total to their asset holdings. Recognizing that our empirical analysis depends heavily on the data sample, we raise two questions around the reliability of the database as a good representation of the actual distribution. First, what can we say about the characteristics and climate exposure of the firms in the JKP23 database that are not matched to any physical assets? Second, for the firms we manage to match to their assets, does our intensity measure reasonably capture their true climate risk?

Sample selection bias. On the first question, Table A7 compares the characteristics of matched and dropped firms side-by-side. The matched sample has a higher median size, a slightly lower book-to-market ratio, a higher operating profitability, and a slightly higher market beta. More importantly, based on the number of firm-months on each side, dropped firms make up a much bigger sample with more than ten times the number of firm-months as matched firms based on financial characteristics. However, more than 90% of the GHG-reporting firms are included in the matched sample, suggesting that the dropped firms generally do not have proper climate risk disclosures.

Error in measurement. On the second question, it is empirically challenging to quantify the error in measurement. However, note that our climate exposure factor (CEF) is an intensity-based measure that does not depend on asset financial value by construction. The equal weighting of

assets assumes assets do not vary substantially in financial value, underlying potential measurement error. To test whether our measure captures climate risk with reasonable relative accuracy, we examine the correlation of our absolute measure CEV with GHG emissions (see Table A5). This is helpful because GHG emissions are a key indicator of firms' operating activities that generate revenue, and firms with higher GHG emissions should have more physical assets on average. The correlation between these two measures is not expected to be one even in the idealistic scenario because GHG emissions are not differentiated by the location of production facilities, which is an important factor in physical risk modeling. Nevertheless, CEV has a correlation of above 45% with total GHG emissions (and above 50% with scope 2 emissions), which gives us assurance that we do not systematically misestimate physical risk exposures across firms in a major way.

Survivorship bias. Another concern of our approach is the backfilling of the asset-level information. We acknowledge that we only utilize point-in-time information of firms' asset locations. As a result, our empirical analysis is subject to survivorship bias that can particularly distort the results for firms in the extreme exposure regime. Firms that have experienced devastating climate damages may have implemented climate adaptations through asset relocations, or encountered critical financial difficulties that eventually led to delisting or even bankruptcy. Our measure underestimates would underestimate the climate exposure at the time in the former case and completely excludes the firms in the latter case. However, large-scale asset relocations to prevent climate impact remain uncommon thus far and the backfilling of more recent asset information generally weakens the estimated effects rather than artificially increase them. On the latter cause, our matched sample does not have a statistically differentiable median return from dropped firms, suggesting that climate-induced credit events remain very unlikely (see Table A7).

V. The Economics of Climate Exposure Premium

The history of climate finance remains brief, whether viewed through the lens of emissions regulation or the incorporation of climate considerations into corporate governance and investment processes. This limited time series poses a significant empirical challenge: backtested

results offer weak support for long-term validity claims. Recognizing this constraint, our physical climate impact assessment framework employs forward-looking climate scenarios to establish an explicit link between climate exposure and expected impact value. However, this value-based exposure measure need not translate linearly into market prices, as markets are noisy and investors operate under heterogeneous motivations and constraints. In her presidential address, Starks (2023) parses corporate sustainability motivations into two fundamental categories: *value*-based and *preference*-based, or in her framing, "*value* versus *values*." This section examines the economic implications of these dual motivations and evaluates whether our empirical findings in Section IV support each underlying mechanism.

A. Climate Risk and Firm Value

Cornell and Damodaran (2023) identify four primary value drivers of corporate sustainability in a discounted cash flow paradigm: revenue growth, operating profitability, investment efficiency, and cost of capital. The first three operate through *cash flows*, while the fourth affects the *discount rates*. Under the cash flow channel, firms with lower exposure sustain long-term growth more reliably, while high-exposure firms face greater cash flow uncertainties. Under the discount rate channel, high-exposure firms command higher risk premiums. Both channels imply that climate-insulated firms are more valuable than climate-exposed firms, ceteris paribus. Consequently, in equilibrium, low-exposure firms should exhibit lower book-to-market ratios and lower expected returns.

Empirical support exists for both channels. Examining cash flows, Darrien et al. (2025) show that negative corporate sustainability news reduces firm value by lowering earnings forecasts. On discount rates, Gormsen, Huber, and Oh (2024) find that low-emission firms command lower cost of capital. However, direct stock market evidence remains mixed (Zhang, 2025), potentially reflecting market inefficiency in pricing climate exposure as investors underreact to climate information.

Building on this literature, our analysis provides direct evidence on the realized pricing of physical climate risk. Using historical records of the thirty most severe flood events in the US, we show that high-exposure firms experience substantial declines in operating profitability, which becomes evident approximately six months post-disaster. Stock prices adjust upon realization of these losses, generating a negative realized climate exposure premium concentrated among directly affected firms. Firms without unrealized exposure, by contrast, do not exhibit persistent return or profitability effects. These results indicate that markets incorporate physical climate risk predominantly *ex post*, highlighting a clear distinction between realized damages and the expected losses captured by our CEF measure. As such, attempts to infer firms' physical climate exposure from historical sensitivities to climate shocks, such as estimating a "climate beta" in the spirit of CRISK (Jung et al., 2025), tend to reproduce patterns driven by realized returns rather than identify the forward-looking exposure captured by our independent CEF measure.

B. Climate Exposure Preferences

Investor demand for climate-resilient assets can generate a distinct pricing channel that is independent of fundamental risk. This preference-based channel has been explored in the literature through both theoretical and empirical work. Dessaint and Matray (2017), Alok, Kumar, and Wermer (2020), and Choi, Gao, and Jiang (2020) document how investor sentiment toward climate and environmental issues affects asset allocation and returns. Pástor, Stambaugh, and Taylor (2021, 2022) provide an equilibrium framework showing that surges in climate concern can temporarily reprice assets based on perceived climate characteristics rather than fundamentals. Similarly, Giglio et al. (2021) demonstrate mean-reverting effects in property markets following climate-event-induced spikes, highlighting that demand-driven adjustments can be significant but transient. Together, these studies suggest that investor climate preferences can create short-term return dynamics that are distinct from value-driven, fundamental adjustments.

Our analysis provides the first direct evidence of a persistent, preference-driven climate exposure premium for physical risk in equity markets. Using the forward-looking CEF measure,

we show that firms with lower physical climate exposure face strong demand from investors, which compresses their expected returns, while high-exposure firms earn higher expected returns as compensation for lower demand. Salient climate events provide evidence of active climate divestment, as heightened investor climate aversion temporarily reallocates capital toward climate-insulated assets. The resulting underperformance of high-exposure firms dissipates as climate exposure preference restores post-disaster, recovering the long-run climate exposure premium.

If the observed premiums reflect preference-driven flows rather than fundamental repricing, why don't informed investors arbitrage away this mispricing? Our results suggest the persistence of preference-induced premiums stems from limits to arbitrage. Survey evidence from Krueger, Sautner, and Starks (2020) indicates that institutional investors increasingly integrate climate considerations into investment decisions through formal mandates and guidelines. Such mandates may constrain climate arbitrage and tilt portfolios away from high-exposure stocks regardless of valuation, sustaining discounts on climate-exposed securities and thus the climate exposure premium.

C. Climate Efficient Frontier under Incomplete Adjustments of Realized Risk

If the market underprices realized climate impact on firms' future profitability, high-exposure firms may be effectively overvalued, yielding lower expected returns than low-exposure firms. While we classify firms into realized and unrealized physical risk *ex post*, real-world investors cannot foresee these outcomes and thus invest in a mix of both groups. In an efficient market where realized climate damages are fully priced, such mixing would not distort expected returns. However, incomplete adjustment for realized climate losses can depress returns on high-exposure firms, generating a hump-shaped relation between risk-adjusted returns and physical climate exposure, rather than a monotonic increase. Pedersen, Fitzgibbons, and Pomorski (2021) document a similar hump-shaped ESG-efficient frontier, where ESG considerations create trade-offs between risk-adjusted returns and sustainability objectives.

We formalize this intuition by constructing a climate-efficient frontier that maps the realized Sharpe ratios across the full spectrum of climate exposure, including firms affected by climate disasters (see Figure 9). The frontier's hump shape captures the underlying mechanism: at moderate exposure levels, preference-driven demand for low-exposure assets compresses expected returns, whereas at extreme exposure levels, incomplete pricing of realized climate losses depresses returns on high-exposure firms.

VI. Conclusion

This paper introduces a ground-up approach to firm-level physical climate risk measurement. We map future climate outcomes projected by climate-economy models to geographically exposed assets to derive a firm-wide overall physical exposure measure. Our measure represents the expected losses of firms' assets over their entire useful life with their future damage rates and uncertainties guided by hazard models and damage functions. Our estimation of the firm-level climate exposure differentiates from works such as Engle et al. (2020) and Sautner et al. (2024) in completely discounting perceived risk measures derived from news, ratings and firms' reports. Our measure is orthogonal to any of these measures with almost zero correlations.

We make three principal contributions. First, we provide a scalable framework to assess firms' climate risk dynamically as asset ownership evolves. Second, we document a statistically and economically significant *ex ante* climate exposure premium driven by investor climate preference. Third, we provide evidence for market reactions to salient climate risks, which tilt short-term capital reallocations in favor of climate safe-haven assets.

References

Albuquerque, R., Koskinen, Y., and Zhang, C. (2019). Corporate social responsibility and firm risk: Theory and empirical evidence, *Management Science* 65(10), 4451–4949.

Alok, S., Kumar, N., and Wermer, R. (2020). Do fund managers misestimate climatic disaster risk, *Review of Financial Studies* 33(3), 1146–1183.

Ardia, D., Bluteau, K., Boudt, K., and Inghelbrecht, K. (2023). Climate change concerns and the performance of green versus brown stocks, *Management Science* 69(12), 7151–7882.

Baldauf, M., Garlappi, L., and Yannelis, C. (2020). Does climate change affect real estate prices? Only if you believe in it. *Review of Financial Studies* 33(3), 1256–1295.

Barro, R.J. (2006). Rare disasters and asset markets in the twentieth century, *Quarterly Journal of Economics* 121(3), 823–866.

Barro, R.J. (2009). Rare disasters, asset prices, and welfare costs, *American Economic Review* 99(1), 243–264.

Barro, R.J., and Jin, T. (2011). On the size distribution of macroeconomic disasters, *Econometrica* 79(5), 1567–1589.

Bernstein, A., Gustafson, M.T., and Lewis, R.C. (2019). Disaster on the horizon: The price effect of sea level rise, *Journal of Financial Economics* 134(2), 253–272.

Bolton, P., Despres, M., Pereira da Silva, L.A., Samama, F., and Svartzman, R. (2020). *The green swan: Central banking and financial stability in the age of climate change*. Bank for International Settlements.

Bolton, P., and Kacperczyk, M. (2021). Do investors care about carbon risk? *Journal of Financial Economics* 142(2), 517–549.

Bolton, P., and Kacperczyk, M. (2023). Global pricing of carbon-transition risk, *Journal of Finance* 78(6), 3677–3754.

Carhart, M.M. (1997). On persistence in mutual fund performance, *Journal of Finance* 52(1), 57–82.

Chava, S. (2014). Environmental externalities and cost of capital, *Management Science* 60(9), 2223–2247.

Choi, D., Gao, Z., and Jiang, W. (2020). Attention to global warming, *Review of Financial Studies* 33(3), 1112–1145.

Cornell, B., and Damodaran, A. (2020) Valuing ESG: Doing good or sounding good? *Journal of Impact and ESG Investing* 1(1), 76–93.

Coronese, M., Lamperti, F., Keller, K., Chiaromonte, F., and Roventini, A. (2019). Evidence for sharp increase in the economic damages of extreme natural disasters, *Proceedings of the National Academy of Sciences* 116(43), 21450–21455.

Deschênes, O., and Greenstone, M. (2007). The economic impacts of climate change: Evidence from agricultural output and random fluctuations in weather, *American Economic Review* 97(1), 354–385.

Dessaint, O., and Matray, A. (2017). Do managers overreact to salient risk? Evidence from hurricane strikes, *Journal of Financial Economics* 126(1), 97–121.

Edmans, A. (2011). Does the stock market fully value intangibles? Employee satisfaction and equity prices, *Journal of Financial Economics* 101(3), 621–640.

Engle, R.F., Giglio, S., Kelly, B., Lee, H., and Stroebel, J. (2020). Hedging climate change news, *Review of Financial Studies* 33(3), 1184–1216.

Fama, E.F., and French, K.R. (1993). Common risk factors in the returns on stocks and bonds, *Journal of Financial Economics* 33(1), 3–56.

Fama, E.F., and French, K.R. (2015). A five-factor asset pricing model, *Journal of Financial Economics* 116(1), 1–22.

Fama, E.F., and MacBeth, J.D. (1973). Risk, return, and equilibrium: Empirical tests, *Journal of Political Economy* 81(3), 607–636.

Gabaix, X. (2012). Variable rare disasters: An exactly solved framework for ten puzzles in macro-finance, *Quarterly Journal of Economics* 127(2), 645–700.

Gibson Brandon, R., Krueger, P., and Mitali, S.F. (2021). The sustainability footprint of institutional investors: ESG driven price pressure and performance, ECGI Working Paper Series in Finance, 571.

Giglio, S., Maggiori, M., Rao, K., Stroebel, J., and Weber, A. (2021). Climate change and long-run discount rates: Evidence from real estate, *Review of Financial Studies* 34(8), 3527–3571.

Gormsen, N.J., Huber, K., and Oh, S. (2024) Climate capitalists, *NBER Working Paper Series*, 32933.

Hong, H., Li, F.W., and Xu, J. (2019). Climate risks and market efficiency, *Journal of Econometrics* 208(1), 265–281.

Hou, K., Xue, C., and Zhang, L. (2015). Digesting anomalies: An investment approach, *Review of Financial Studies* 28(3), 650–705.

Huizinga, J., De Moel, H., Szewczyk, W. (2017). *Global flood depth-damage functions – Methodology and the database with guidelines*. Joint Research Centre, European Commission.

Intergovernmental Panel on Climate Change (IPCC). (2012). Determinants of risk: Exposure and vulnerability, in *Managing the risks of extreme events and disasters to advance climate change adaptation*. Cambridge University Press.

Intergovernmental Panel on Climate Change (IPCC). (2022). Summary for Policymakers, in *Climate change 2022: Impacts, adaptation and vulnerability*. Cambridge University Press.

Jensen, T.I., Kelly, B.T., and Pedersen, L.H. (2023). Is there a replication crisis in finance? *Journal of Finance* 78(5), 2465–2518.

Jung, H., Engle, R.F., and Berner, R. (2025). CRISK: Measuring the climate risk exposure of the financial system, *Journal of Financial Economics* 171, 104076.

Krueger, P., Sautner, Z., and Starks, L.T. (2020). The importance of climate risks for institutional investors, *Review of Financial Studies* 33(3), 1057–1111.

Kou, S. (2002). A jump-diffusion model for option pricing, *Management Science* 48(8), 1086–1101.

Mehra, R., and Prescott, E.C. (1985). The equity premium: A puzzle, *Journal of Monetary Economics* 15(2), 145–161.

Merton, R.C. (1974). On the pricing of corporate debt: The risk structure of interest rates, *Journal of Finance* 29(2), 449–470.

Merton, R.C. (1976). Option pricing when underlying stock returns are discontinuous, *Journal of Financial Economics* 3(1–2), 125–144.

Nordhaus, W.D. (1991). To slow or not to slow: The economics of the greenhouse effect, *Economic Journal* 101(407), 920–937.

Pástor, L'., Stambaugh, R.F., and Taylor, L.A. (2021). Sustainable investing in equilibrium, *Journal of Financial Economics* 142(2), 550–571.

Pástor, L'., Stambaugh, R.F., and Taylor, L.A. (2022). Dissecting green returns, *Journal of Financial Economics* 146(2), 403–424.

Pedersen, L.H., Fitzgibbons, S., and Pomorski, L. (2021). Responsible investing: The ESG-efficient frontier, *Journal of Financial Economics* 142(2), 572–597.

Prankratz, N.M.C., and Schiller, C.M. (2024). Climate change and adaptation in global supply-chain networks, *Review of Financial Studies* 37(6), 1729–1777.

Sautner, Z., van Lent, L, Vilkov, G., and Zhang, R. (2023). Firm-level climate change exposure, *Journal of Finance* 78(3), 1449–1498.

Starks, L.T. (2023). Presidential address: Sustainable finance and ESG issues – *value* versus *values*, *Journal of Finance* 78(4), 1837–1872.

Ward, P.J., Winsemium, H.C., Kuzma, S., Bierkens, M.F.P., Bouwman, A., De Moel, H., Loaiza, A.D., Eilander, D., Englhardt, J., Erkens, G., Gebremedhin, E.T., Iceland, C., Kooi, H., Ligtvoet, W., Muis,

S., Scussolini, P., Sutanudjaja, E.H., Van Beek, R., Van Bemmel, B., Van Huijstee, J., Van Rijn, F., Van Wesenbeeck, B., Vatvani, D., Verlaan, M., Tiggeloven, T., and Luo, T. *Aqueduct floods methodology*. World Resources Institute.

Zhang, S. (2025). Carbon returns across the globe, *Journal of Finance* 80(1), 615–645.

Appendix I. Estimation of Asset-Level Climate Damage Distribution

This section explains the implementation of maximum likelihood estimation for the log damage rate distribution for the asset process (Eq. 6). The purpose of this estimation is to use probability distributions with a tractable moment generating function to approximate the original Gumbel distribution derived in Section III.

The log damage $J_t \sim Gumbel(\kappa\mu_G, \kappa\beta_G)$ is derived based on climate hazard intensity distribution $Gumbel(\mu_G, \beta_G)$ scaled by the asset vulnerability factor κ. We simulate a random sample of J_t and use the sample to estimate the parameters of the target distributions. In this section, we study two target distribution: (a) normal distribution for Merton jump process, and (b) hybrid normal-exponential distribution for our suggested jump process in this paper.

A. Merton Jump Distribution

A Merton (1976) jump process assumes Gaussian $J_t \sim N(\mu_N, \sigma_N^2)$, such that

$$E[\exp(-J)] = \exp\left(-\mu_N + \frac{1}{2}\sigma_N^2\right) \tag{A1}$$

and $Var[V_T]$ remains analytically tractable, making V_T lognormally distributed. The normal-distributed jumps can be estimated using the sample mean and variance of the simulated sample

$$\hat{\mu}_N = \frac{1}{n}\sum_{i=1}^{n} J_i\,, \qquad \hat{\sigma}_N^2 = \frac{1}{n-1}\sum_{i=1}^{n}(J_i - \hat{\mu}_J)^2 \tag{A2}$$

with the method of moments.

B. Normal-Exponential Hybrid Jump Distribution

We suggest a hybrid distribution with a normal core and an exponential tail to optimize the empirical fit for the hazard intensity distribution and ensure computational tractability. Eq. 9 characterizes the density function of the hybrid distribution. We first set a right tail probability p, and the simulated sample can be split into a normal side $I_1 = \{i : \ j_i \leq J_p\}$ and an exponential side $I_2 = \{i : \ j_i > J_p\}$. The log-likelihood of this hybrid distribution is given as

$$\ln \mathcal{L}(\mu_N, \sigma_N^2, \eta)$$

$$= \sum_{i \in I_1} \ln \left[\frac{1-p}{\sigma_N} \frac{\phi((j_i - \mu_N)/\sigma_N)}{\Phi((J_p - \mu_N)/\sigma_N)} \right] + \sum_{i \in I_2} \ln \left[p\eta \exp\left(-\eta(j_i - J_p)\right) \right] \quad \text{(A3)}$$

$$= n_1 \ln(1-p) - n_1 \ln \sigma_N - n_1 \ln\left(\Phi((J_p - \mu_N)/\sigma_N)\right) - \frac{n_1}{2}\ln(2\pi)$$

$$- \sum_{i \in I_1} \frac{1}{2}((j_i - \mu_N)/\sigma_N)^2 \ + n_2 \ln p + n_2 \ln \eta - \eta \sum_{i \in I_2} (j_i - J_p)$$

where η is given by Eq. 10 to ensure continuity of the density function at J_p. Since the log likelihood function is not convex, we optimize it using a limited-memory BFGS algorithm with initial parameter values for $\hat{\mu}_N$ and $\hat{\sigma}_N^2$ chosen as the sample mean and variance in Eq. A2. The algorithm is a quasi-Newton method that approximates the Hessian matrix and iteratively converges to a local maximum. The initial parameter values are selected based on the fact that a vanilla normal distribution overestimates the peak density (or mode of the density function) due to the heavy tail. Intuitively, we can start with these estimates for a Merton jump and gradually pivots left-ward to the optimum. See Figure 3 for the optimized parameters for (a) Merton and (b) hybrid jumps. Compared to the vanilla normal density curve, the normal core of the hybrid distribution indeed shifts left-ward towards the peak of the empirical distribution.

Figure 1
Physical Asset Geospatial Distribution

This figure displays the number of physical assets mapped to each US county by asset longitude and latitude. Locations of assets are mapped to administrative divisions in the US (country-state-county) using a geocoder via maps from GADM. Assets with no longitude and latitude information and those with mislabeled longitude or latitude are removed from the sample. These include assets that are misassigned to the centroid of the country.

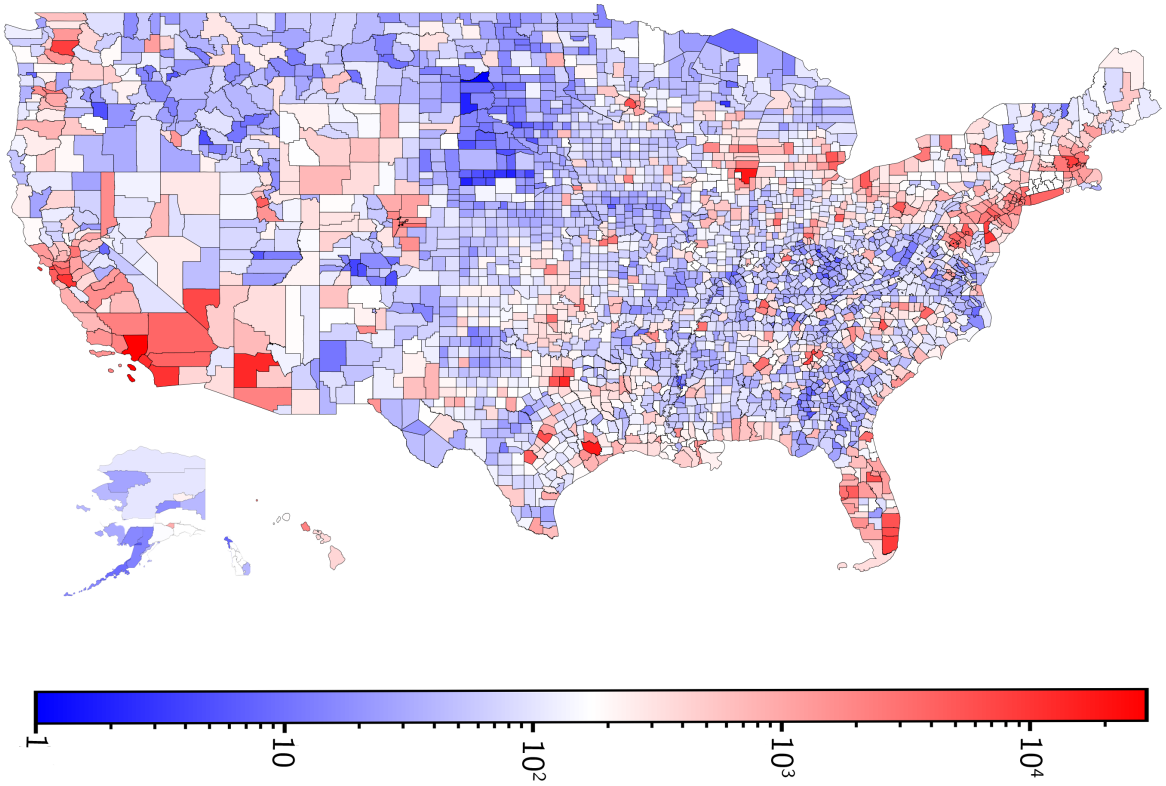


Figure 2
Fitted Flood Damage Curves

This figure plots the fractional damage factor as a function of flood depth in meters for six major types of physical assets in the United States. The scatters marked by crosses are historical observations sourced from the EU JRC global flood depth-damage database. The smooth fitted lines represent damage curves with an exponential CDF form. Our stylized asset-level damage function is a concave function defined for positive hazard intensities and bounded in [0, 1]. While empirical results suggest a non-zero damage factor when flood depth is zero for certain asset classes, we force the damage curve to start from the origin to be consistent with our jump-diffusion setup, where a hazard intensity of zero signals no occurrence of hazard and therefore causes no damage to the asset. To ensure optimal fit for physical assets studied in this paper, we calibrate the exponential CDF damage function by adding weights to the scatters equal to their respective numbers of exposed assets projected by WRI Aqueduct flood maps. The calibrated parameters and calibration fit are summarized in Table A1.

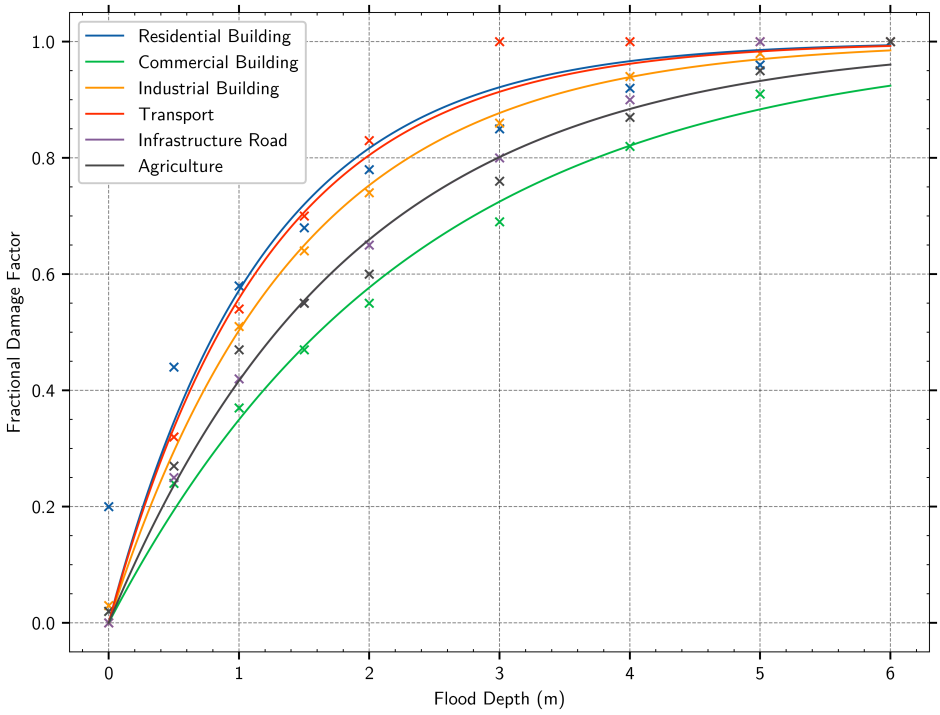


Figure 3

Future Coastal Flood Damage Distribution Calibrated for Merton and Hybrid Jumps

This figure plots histograms of Gumbel-distributed log damage rate J due to coastal flood and parametrized probability density curves. The sample is generated for a (location-wise) median US coastal flood event in 2030, 2050 and 2080 using inundation maps projected under the business-as-usual (RCP8.5) scenario. We assume an asset vulnerability $\kappa = 0.699$ (equivalent to industrial building, see Table A1). The log jump size is re-parametrized in two ways: (a) Merton jumps that are normally distributed, or (b) hybrid jumps with a normal core (blue dashdotted) and an exponential tail (red dashed). For the hybrid distribution, we set a cutoff right tail probability $p = 0.3$ (cutoff quantile J_p marked as a red circle).

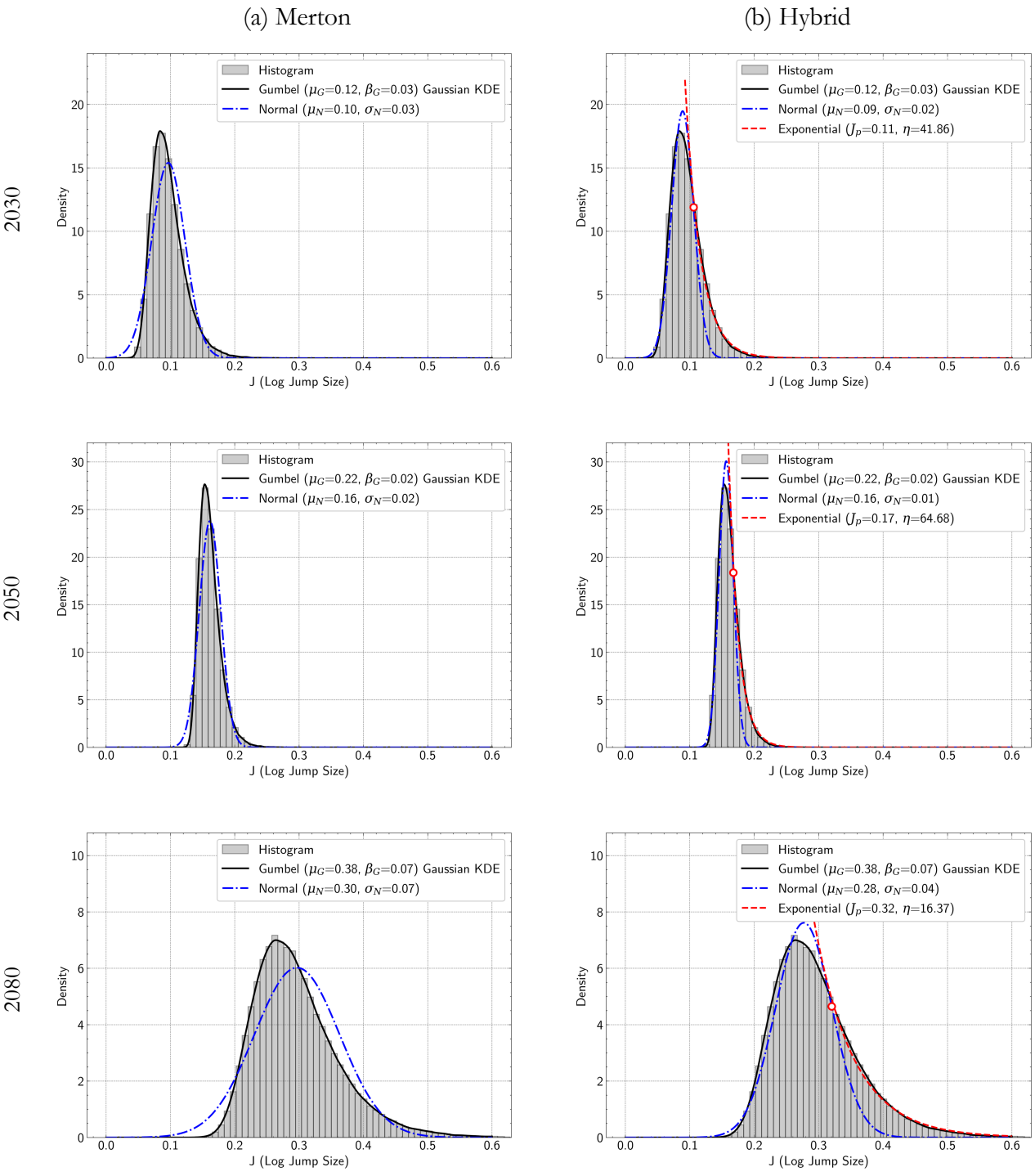


Figure 4

Future Riverine Flood Damage Distribution Calibrated for Merton and Hybrid Jumps

This figure plots histograms of Gumbel-distributed log damage rate J due to riverine flood and parametrized probability density curves. The sample is generated for a (location-wise) median US riverine flood event in 2030, 2050 and 2080 using inundation maps projected under the business-as-usual (RCP8.5) scenario. We assume an asset vulnerability $\kappa = 0.699$ (equivalent to industrial building, see Table A1). The log jump size is re-parametrized in two ways: (a) Merton jumps that are normally distributed, or (b) hybrid jumps with a normal core (blue dashdotted) and an exponential tail (red dashed). For the hybrid distribution, we set a cutoff right tail probability $p = 0.3$ (cutoff quantile J_p marked as a red circle).

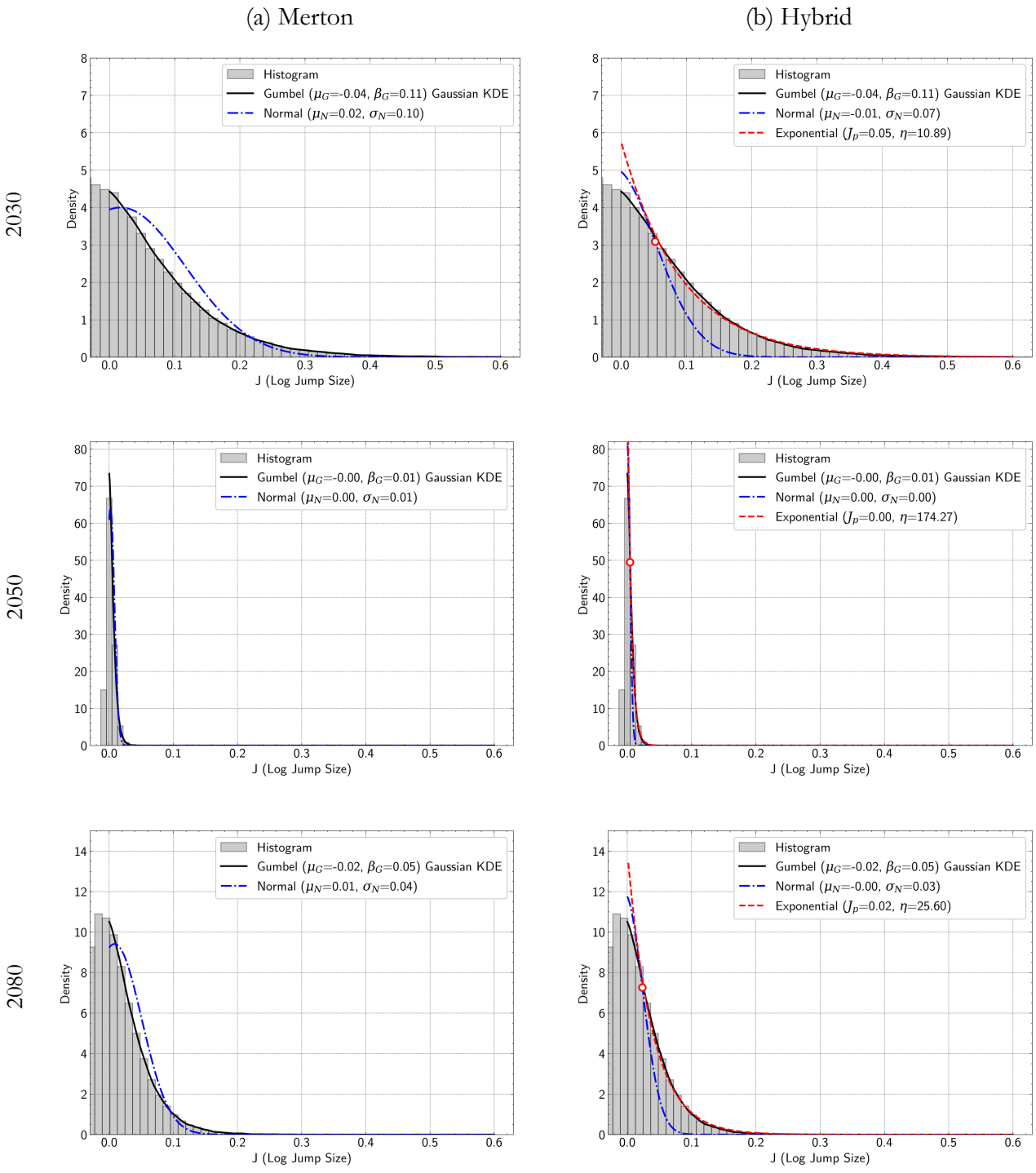


Figure 5
Asset Forward Annual Retention Rate

This figure plots time series of the expected annual retention rate $M_J(t)$ from flood events in the US. All retention rates are estimated under the business-as-usual (RCP8.5) scenario. We first estimate the retention rates due to (a) coastal flood, and (b) riverine flood in 2030, 2050 and 2080 based on Eq. 11. Then, we apply linear interpolation to the remaining data points illustrated in the graphs. The whisker plot illustrates the retention rates of US assets within 1 standard deviation from their average.

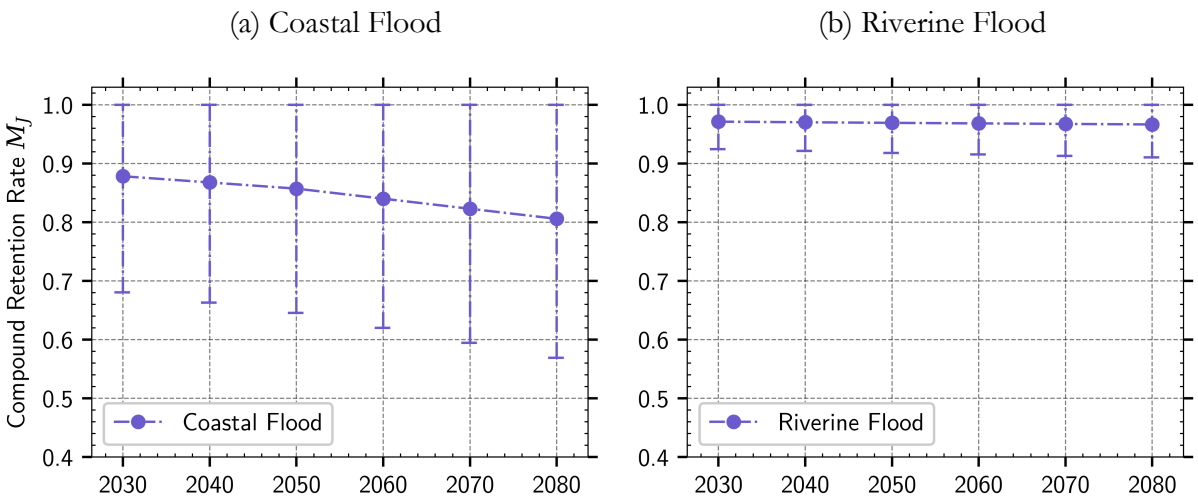


Figure 6
Asset Cumulative Retention Factor

This figure plots time series of cumulative retention factor from flood events in the US. The factor measures asset depreciation from climate disasters and is calculated as $\exp(\int_{T_0}^{T}(M_J(t)-1)\lambda dt)$, setting $\lambda = 1$, $T_0 = 2030$ and $M_J = 1$ at T_0. We first estimate the retention rates due to (a) coastal flood, and (b) riverine flood in 2030, 2050 and 2080 based on Eq. 11. Then, we apply linear interpolation to the remaining data points illustrated in the graphs. We illustrate for both business-as-usual (RCP8.5, blue dotted) and intermediate transition (RCP4.5, green dashed) scenarios.

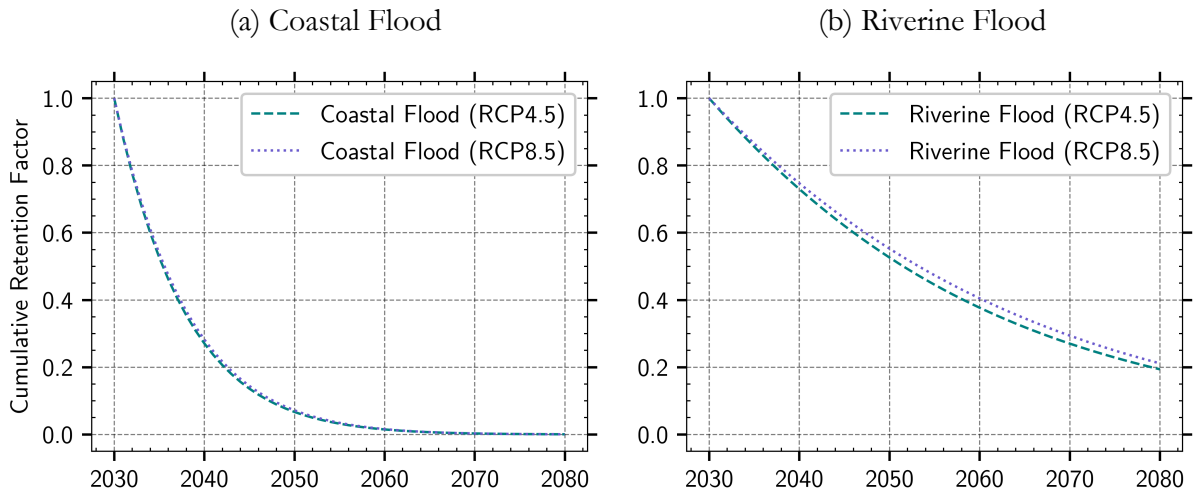


Figure 7
Empirical Climate Exposure Premium

This figure presents the CEF return spread curve estimated using CEF decile portfolios (in Table 3) and a Fama-MacBeth regression (in Table 5). The blue curve illustrates a quadratic spline fitted to (a) equally weighted and (b) value-weighted CEF decile portfolio averages (blue scatters). The teal dotted line is estimated using a Fama-MacBeth OLS model where firm excess returns are regressed against CEF and CEF-squared (to account for curvature), controlling for variables described in Table 5. In each year, monthly excess returns of individual firms from April to next March are regressed against lagged firm characteristics collected by the end of this March. Both portfolio sort and Fama-MacBeth OLS adjust for industry effects based on GICS (2-digit GIC for portfolio sort and 4-digit GIC for OLS industry fixed effects). CEF spread is measured as portfolio/firm returns subtracted by the first decile portfolio R_0, which has a zero CEF. The sample period is September 2003 to March 2024. Returns are annualized by multiplying the monthly returns by 12.

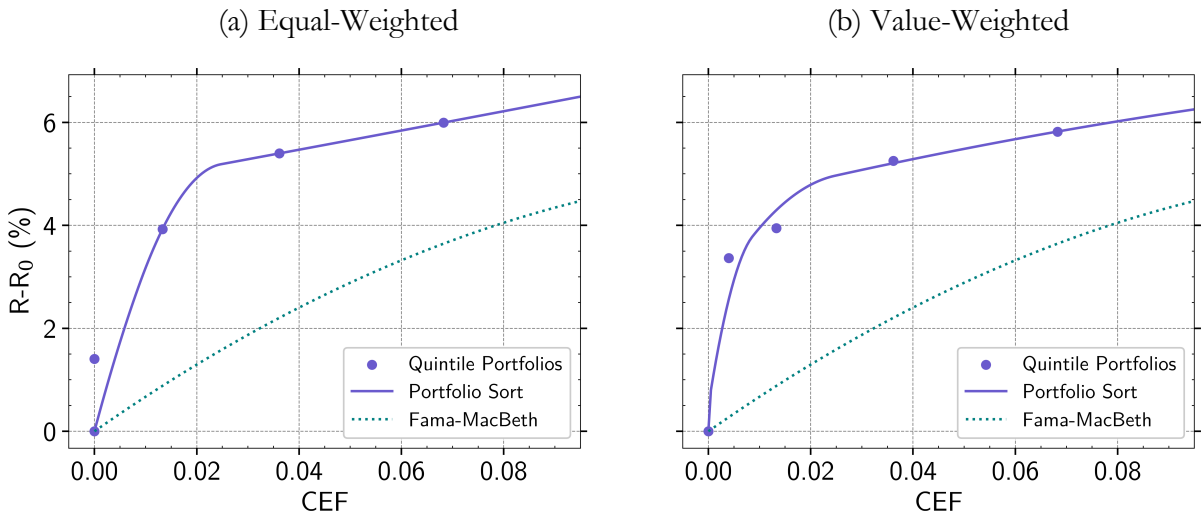


Figure 8
Exposed-Minus-Insulated (EMI) Portfolio Returns

This figure plots time series of exposed-minus-insulated (EMI) portfolio returns from September 2003 to March 2024. We follow the Fama-French approach by simultaneously buying top 1/3 and selling bottom 1/3 of the CEF-sorted firms using the method in Table 4. The mimicking portfolio value-weights constituent stock returns within the tercile. We smooth the EMI returns by taking the 12-month rolling mean of the original monthly returns series. The red dotted line denotes the average monthly return of the EMI portfolio during the sample period. Returns are annualized by multiplying the monthly returns by 12.

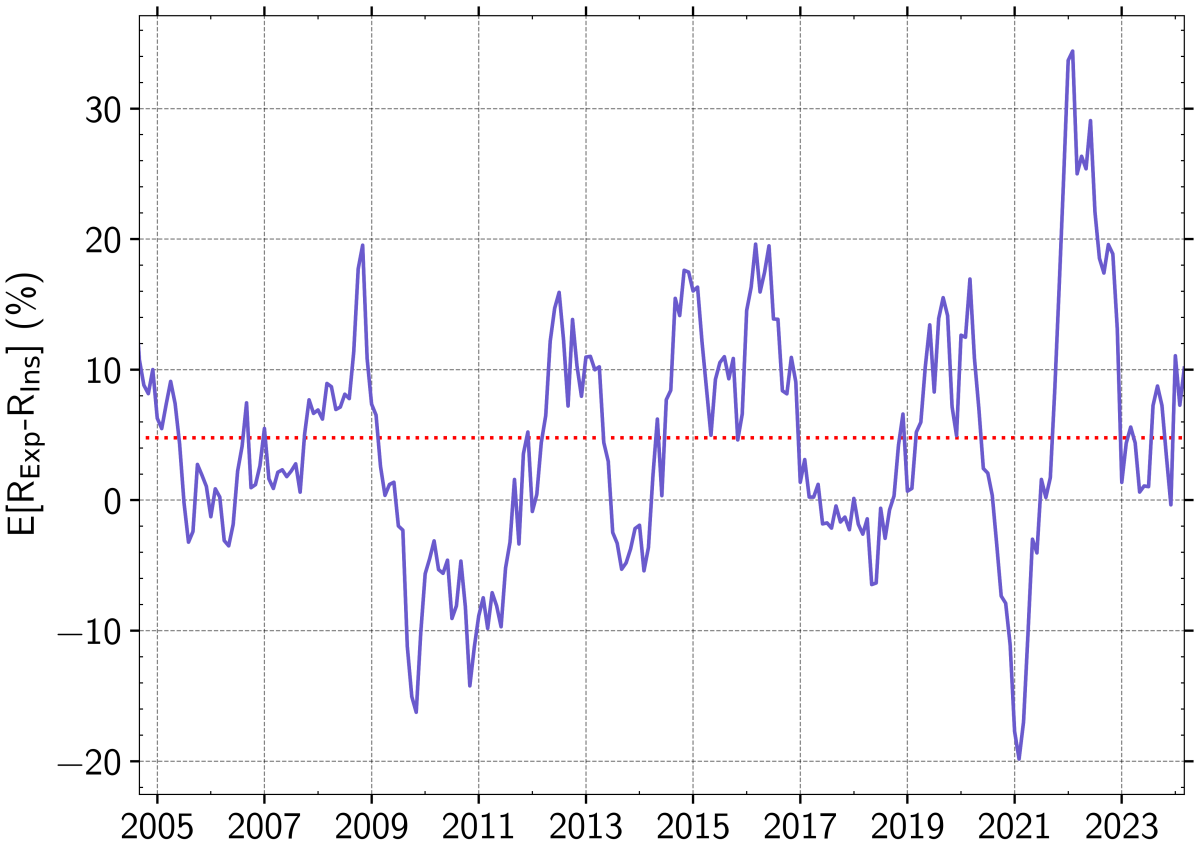


Figure 9
Climate Efficient Frontier

This figure presents a climate efficient frontier that indicates the highest attainable Sharpe ratio given a climate exposure level using S&P 500 constituent stock returns from April 2012 to March 2024. Climate risk is measured using CEF. The climate-integrated tangency portfolio is marked as a round dot in dark blue. The realized climate-efficient frontier is illustrated in a cross-patterned curve, which represents the optimal Sharpe ratio with the lowest possible climate exposure.

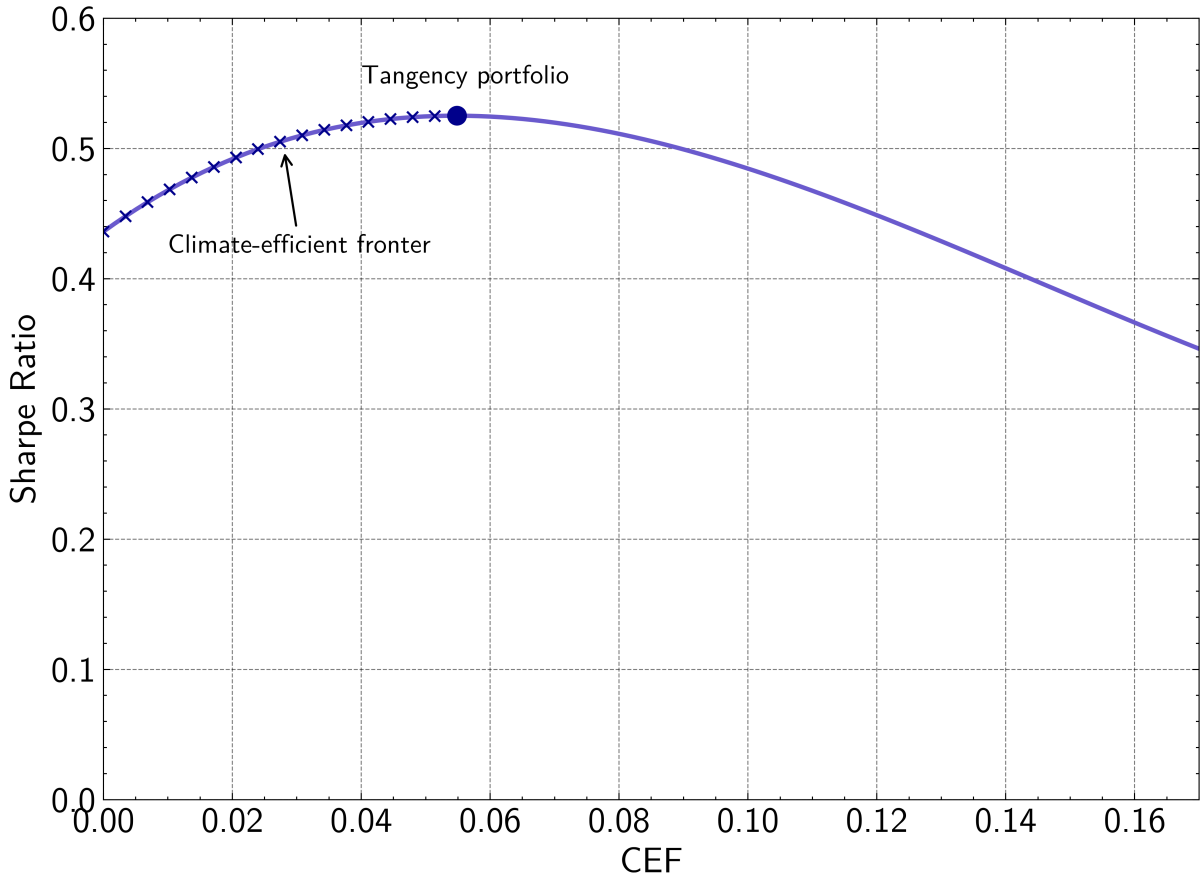


Table 1
Asset Climate Exposure Summary Statistics

This table documents the summary statistics for the average annual retention rate from flood events $\overline{M}_J(-1)$ by asset type. Panel A reports the average retention factors from 2030 to 2080 with linear interpolation under the business-as-usual (RCP8.5) scenario, while Panel B reports the values under the intermediate transition (RCP4.5) scenario. The full sample of assets can be divided into exposed and unexposed assets, where only exposed assets are affected by flood events according to our hazard distribution. The mean, median and standard deviation are calculated among all exposed assets.

	Total	Unexposed	Exposed				
	Obs	Obs	Obs	Pct	Mean	Median	Std. Dev.
Panel A: Business-as-Usual (RCP8.5) Scenario							
Coastal Flood							
Commercial	886,087	881,680	4,407	0.5%	0.831	0.975	0.219
Industrial	95,832	94,575	1,257	1.3%	0.890	0.974	0.173
Infrastructure	208,763	207,674	1089	0.5%	0.879	0.984	0.203
Residential	34,071	33,836	235	0.7%	0.743	0.880	0.289
Agriculture	24	24	0	0%	-	-	-
Total	1,224,777	1,217,789	6,988	0.6%	0.846	0.975	0.214
Riverine Flood							
Commercial	886,087	778,360	107,727	12.2%	0.972	0.989	0.045
Industrial	95,832	86,530	9,302	9.7%	0.945	0.972	0.072
Infrastructure	208,763	187,189	21,574	10.3%	0.965	0.985	0.057
Residential	34,071	29,518	4,553	13.4%	0.956	0.983	0.069
Agriculture	24	16	8	33.3%	0.966	0.972	0.032
Total	1,224,777	1,081,613	143,164	11.7%	0.969	0.987	0.051
Total							
Commercial	886,087	776,353	109,734	12.4%	0.966	0.988	0.069
Industrial	95,832	85,960	9,872	10.3%	0.934	0.970	0.097
Infrastructure	208,763	186,683	22,080	10.6%	0.960	0.983	0.075
Residential	34,071	29,416	4,655	13.7%	0.944	0.979	0.106
Agriculture	24	16	8	33.3%	0.966	0.972	0.032
Total	1,224,777	1,078,428	146,349	11.9%	0.962	0.985	0.074
Panel B: Intermediate Transition (RCP4.5) Scenario							
Coastal Flood							
Commercial	886,087	881,886	4,201	0.5%	0.830	0.979	0.219
Industrial	95,832	94,608	1,224	1.3%	0.898	0.978	0.167
Infrastructure	208,763	207,731	1,032	0.5%	0.882	0.985	0.203
Residential	34,071	33,846	225	0.7%	0.749	0.878	0.291
Agriculture	24	24	0	0%	-	-	-
Total	1,224,777	1,218,095	6,682	0.5%	0.848	0.979	0.213
Riverine Flood							
Commercial	886,087	778,977	107,110	12.1%	0.971	0.987	0.046
Industrial	95,832	86,527	9,305	9.7%	0.942	0.967	0.074
Infrastructure	208,763	187,330	21,433	10.3%	0.962	0.983	0.059
Residential	34,071	29,555	4,516	13.3%	0.953	0.978	0.071
Agriculture	24	17	7	29.2%	0.953	0.963	0.041
Total	1,224,777	1,082,406	142,371	11.6%	0.967	0.986	0.052
Total							
Commercial	886,087	777,095	108,992	12.3%	0.965	0.986	0.068
Industrial	95,832	85,990	9,842	10.3%	0.933	0.967	0.097
Infrastructure	208,763	186,871	21,892	10.5%	0.958	0.982	0.076
Residential	34,071	29,462	4,609	13.5%	0.942	0.978	0.105
Agriculture	24	17	7	29.2%	0.953	0.963	0.041
Total	1,224,777	1,079,435	145,342	11.9%	0.961	0.985	0.074

Table 2
Firm Summary Statistics and Correlations

This table reports summary statistics in Panel A and a correlation matrix in Panel B for firms' climate exposures and financials. CEV (or climate exposure value) is the absolute book value of expected loss due to climate disasters (measured in 2011 millions USD) expressed in Eq. 12, and CEF (or climate exposure factor) is the intensity-based climate exposure measure defined in Eq. 13. The rest of the table are firms' financials reported between September 2003 and March 2024 with monetary terms in 2011 millions USD. ME is market capitalization. B/M is the ratio of book equity to market equity. ROE is operating income before depreciation (EBITDA) scaled by book equity. I/A is the ratio of capital expenditure (item CAPX) to total assets (AT). K/A is the ratio of fixed assets to total assets. S/A is annual sales divided by total assets. Lev (or leverage) is calculated as debt to total assets. We document summary statistics including mean, standard deviation, 5th percentile, 25th percentile, median, 75th percentile, 95th percentile, and the number of firm-months (subject to duplicate financials in each quarter). All variables are winsorized at the 1st and 99th percentiles to exclude extreme outliers.

Panel A: Summary Statistics

	CEF	CEV	ME	B/M	ROE	I/A	K/A	S/A	Lev
Mean	0.04	63.53	7,102.84	0.74	0.14	0.04	0.20	0.77	0.23
Std. Dev.	0.06	242.58	22,801.30	0.98	0.75	0.05	0.23	0.74	0.24
P5	0.00	0.00	17.62	0.07	−0.77	0.00	0.00	0.01	0.00
P25	0.00	0.00	151.85	0.26	0.08	0.01	0.03	0.20	0.04
Median	0.02	1.22	751.44	0.50	0.21	0.02	0.11	0.60	0.17
P75	0.05	15.75	3,620.54	0.87	0.33	0.04	0.29	1.11	0.35
P95	0.16	313.86	32,951.19	2.09	0.78	0.13	0.74	2.23	0.68
N	663,303	625,230	661,502	610,804	589,790	634,618	625,183	640,567	643,259

Panel B: Correlation

	CEF	CEV	ME	B/M	ROE	I/A	K/A	S/A	Lev
CEF	1	0.17	0.03	−0.02	−0.01	−0.07	−0.06	−0.09	−0.04
CEV		1	0.58	0.00	0.09	0.12	0.26	−0.03	0.09
ME			1	−0.10	0.12	0.01	0.03	−0.03	0.06
B/M				1	−0.02	−0.01	0.09	−0.09	0.05
ROE					1	0.07	0.10	0.18	0.14
I/A						1	0.66	0.15	0.10
K/A							1	0.10	0.25
S/A								1	0.03
Lev									1

Table 3
Univariate Portfolio Sorting

This table summarizes the performance of climate exposure factor (CEF) sorted portfolios and spreads. These portfolios are constructed each year by sorting on firms' CEF in March (sort by 1-year lagged CEF for returns in March). Panel A summarizes the average quintile portfolio returns and spreads, standard deviations and t-stats. The portfolios are value-weighted every month. Returns (in %) are annualized by multiplying the monthly returns by 12. *t*-stat is estimated by assuming a zero mean return. We perform time-series regressions of these portfolios against common risk factors with results shown in Panels B, C, and D. Panel B includes value-weighted market excess returns (MKT-RF), size (SMB) and value (HML) factors from Fama and French (1993) plus momentum (MOM) from Carhart (1997). Panel C adds profitability (RMW) and investment (CMA) factors from Fama and French (2015). Panel D uses the *q*-factor model investment (I/A) and profitability (ROE) factors from Hou, Xue, and Zhang (2015). Alpha is the time-series regression intercept. Robust *t*-statistics are in parentheses, with standard errors estimated using Newey-West correction for 12 lags. The sample period is September 2003 to March 2024.

	(Low) 1	2	3	4	(High) 5	H-L
Panel A: Average Monthly Returns						
E[R]-RF	5.21	8.57	9.15	10.46	11.02	5.82
	(1.31)	(1.92)	(2.35)	(3.10)	(3.65)	(3.25)
Std. Dev.	18.39	19.37	17.68	16.20	14.84	8.32
SR	0.28	0.44	0.52	0.65	0.74	0.70
Panel B: Regression on FF3+MOM						
Alpha	−4.56	−2.07	−1.44	0.56	1.56	6.13
	(−3.61)	(−1.36)	(−1.49)	(0.87)	(2.06)	(4.19)
MKT-RF	0.97	1.05	1.06	1.01	0.95	−0.02
	(27.10)	(24.42)	(25.75)	(62.28)	(54.26)	(−0.52)
SMB	0.46	0.51	0.14	−0.05	−0.06	−0.52
	(8.46)	(7.92)	(3.19)	(−2.52)	(−2.05)	(−8.95)
HML	−0.10	−0.10	0.07	0.15	0.03	0.13
	(−1.89)	(−1.63)	(2.65)	(5.16)	(0.99)	(2.35)
MOM	−0.11	−0.08	−0.04	−0.08	0.00	0.11
	(−3.58)	(−4.42)	(−2.26)	(−4.79)	(−0.17)	(3.89)
Adj R^2	0.89	0.92	0.94	0.98	0.94	0.37
Panel C: Regression on FF5						
Alpha	−3.60	−1.77	−1.23	0.37	1.57	5.17
	(−2.47)	(−1.44)	(−1.26)	(0.52)	(1.78)	(3.26)
MKT-RF	0.98	1.05	1.06	1.02	0.95	−0.03
	(35.48)	(27.15)	(28.04)	(57.01)	(58.34)	(−0.79)
SMB	0.40	0.50	0.13	−0.04	−0.06	−0.45
	(6.85)	(9.29)	(2.59)	(−1.99)	(−2.07)	(−7.18)
HML	0.03	0.04	0.15	0.20	0.02	−0.01
	(0.61)	(0.72)	(3.89)	(5.34)	(0.57)	(−0.18)
RMW	−0.25	−0.05	−0.04	−0.01	−0.01	0.24
	(−3.55)	(−0.51)	(−0.78)	(−0.39)	(−0.30)	(2.63)
CMA	−0.19	−0.30	−0.15	−0.06	0.03	0.21
	(−2.71)	(−3.46)	(−2.27)	(−1.51)	(0.57)	(3.93)
Adj R^2	0.89	0.92	0.94	0.97	0.94	0.38

Table 3
(Continued)

	(Low) 1	2	3	4	(High) 5	H-L
	Panel D: Regression on HXZ					
Alpha	−3.66	−1.59	−1.58	0.24	1.28	4.94
	(−2.75)	(−1.33)	(−1.61)	(−0.38)	(1.58)	(3.32)
MKT-RF	0.96	1.04	1.08	1.04	0.96	0.01
	(32.22)	(22.41)	(25.46)	(52.52)	(66.88)	(0.16)
SMB	0.38	0.48	0.17	−0.02	−0.04	−0.42
	(5.92)	(10.17)	(2.93)	(−0.50)	(−1.17)	(−6.29)
I/A	−0.14	−0.23	0.02	0.16	0.05	0.18
	(−2.75)	(−1.33)	(−1.61)	(0.38)	(1.58)	(3.32)
ROE	−0.22	−0.09	−0.02	−0.05	0.04	0.25
	(−3.18)	(−1.30)	(−0.54)	(−1.40)	(1.19)	(3.58)
Adj R^2	0.89	0.92	0.94	0.97	0.94	0.40

Table 4
Portfolio Firm Characteristics

This table reports the time-series average of the median firm characteristics for climate exposure factor (CEF) sorted portfolios in Table 3. Firm characteristics are measured in 2011 million USD as explained in Table 1. Log ME is the natural logarithm of market equity. Beta is the CAPM beta estimated in a 5-year rolling window. $\Delta S/S$ and $\Delta K/K$ are the annual growth rate of sales and physical assets respectively. N is the number of constituent firms in the portfolio. The sample period is September 2003 to March 2024.

	(Low) 1	2	3	4	(High) 5
CEF	0.00	0.00	0.01	0.04	0.07
CEV	0.00	0.00	1.11	9.68	14.30
Log ME	5.26	5.65	6.99	7.81	7.41
B/M	0.57	0.56	0.52	0.50	0.50
ROE	0.13	0.17	0.22	0.25	0.23
I/A	0.02	0.02	0.02	0.02	0.02
K/A	0.11	0.13	0.13	0.12	0.11
S/A	0.60	0.65	0.67	0.69	0.69
Lev	0.10	0.11	0.19	0.23	0.20
Beta	1.06	1.03	1.08	1.02	1.05
$\Delta S/S$	0.07	0.07	0.07	0.07	0.07
$\Delta K/A$	0.01	0.02	0.02	0.02	0.02
N	358	352	352	352	356

Table 5
Fama-MacBeth Regression

This table documents the time-series average of month-by-month cross-sectional regressions of stock excess returns on firms' climate exposure factor (CEF) and other financial characteristics following Fama and MacBeth (1973). In each year, monthly excess returns of individual firms from April to next March are regressed against lagged firm characteristics collected by the end of this March. Like in Table 4, firm characteristics are measured in 2011 millions USD. Log ME is the natural logarithm of firm size. Log B/M is the natural logarithm of book-to-market ratio. ROE is a profitability ratio expressed as operating income (item EBITDA) divided by book equity. I/A is an investment ratio expressed as capital expenditure divided by total assets. K/A is a firm asset tangibility measure defined as total net physical assets (item PPEN) scaled by total assets. Lev is the book leverage ratio given as total debt-to-asset. Beta is the 5-year rolling CAPM beta coefficient. ΔS/S and ΔK/K are the annual growth rate of sales and physical assets respectively. Columns (4) – (6) add industry fixed effects based on the GIC 4-digit classification. Observations are the total number of firm-months in the sample. The sample period is September 2003 to March 2024. All variables are winsorized at the 1st and 99th percentiles to account for extreme outliers. All explanatory variables are cross-sectionally normalized to zero mean and unit standard deviation. Robust *t*-statistics are in parentheses, with standard errors estimated using Newey-West correction for 12 lags. ***1% significance; **5% significance; *10% significance.

	(1)	(2)	(3)	(4)
CEF	1.06***	1.07***	1.08***	1.05***
	(3.84)	(4.05)	(4.04)	(4.31)
Log ME	0.84	0.92	0.87	0.92
	(0.49)	(0.55)	(0.52)	(0.55)
Log B/M	2.41*	2.65**	1.87	2.22**
	(1.92)	(2.51)	(1.63)	(2.29)
ROE	1.64**	1.45**	1.52**	1.33**
	(2.30)	(2.31)	(2.26)	(2.24)
I/A	0.05	−0.05	−0.36	−0.41
	(0.06)	(−0.09)	(−0.43)	(−0.55)
K/A			0.85	0.75
			(0.87)	(0.91)
Lev			0.42	0.55
			(0.74)	(1.12)
Beta			0.83	0.45
			(0.67)	(0.44)
ΔS/S			−0.84***	−0.61*
			(−2.56)	(−1.93)
ΔK/A			−0.47	−0.16
			(−0.90)	(−0.42)
Industry FE	No	Yes	No	Yes
Adj R^2	0.03	0.07	0.04	0.08
Observations	428,666	428,666	428,666	428,666

Table 6
Climate Exposure Premium and Public Attention

This table presents the time-series regression of climate exposed-minus-insulated (EMI) spread against climate media coverage index and macroeconomic signals. The time series of EMI portfolio returns is illustrated in Figure 8. We use the media climate change index from Ardia et al. (2023) as our climate news index (CNI) and test whether the return spread reacts to changes in public attention to climate change, including three specific indices for media coverage of global warming (Phy), policy actions (Reg), and decarbonization technologies (Tech). The macroeconomic signals include default spread (DEF), term spread (TERM), as well as changes in market volatility index (VIX) and University of Michigan consumer sentiment index (CSENT). Columns 1–3 are contemporaneous monthly regressions, and columns 4–6 use lagged climate attention and macro signals. *t*-statistics are in parentheses. The sample period is from September 2003 to March 2024. ***1% significance; **5% significance; *10% significance.

	EMI_t			EMI_{t+1}		
	(1)	(2)	(3)	(4)	(5)	(6)
Alpha	10.12*	10.07*	9.74*	17.12***	17.38***	17.47***
	(1.91)	(1.89)	(1.84)	(3.81)	(3.85)	(3.87)
ΔCNI_t^{Phy}	−15.04***			12.81**		
	(−3.10)			(2.13)		
ΔCNI_t^{Reg}		−10.11*			6.56	
		(−1.67)			(1.39)	
ΔCNI_t^{Tech}			−11.57*			4.53
			(−1.70)			(0.97)
DEF_t	−4.97	−4.73	−4.64	−13.12***	−13.39***	−13.42***
	(−1.01)	(−0.96)	(−0.94)	(−3.11)	(−3.16)	(−3.18)
$TERM_t$	−0.06	−0.17	−0.06	0.68	0.71	0.69
	(−0.04)	(−0.12)	(−0.04)	(0.43)	(0.45)	(0.43)
ΔVIX_t	1.31**	1.32**	1.36**	0.82	0.81	0.80
	(2.00)	(2.06)	(2.15)	(1.57)	(1.53)	(1.50)
$\Delta CSENT_t$	−0.26	−0.35	−0.38	−0.31	−0.23	−0.19
	(−0.54)	(−0.65)	(−0.72)	(−0.79)	(−0.59)	(−0.52)

Table 7
Flood Event Studies

This table documents the pooled regressions on firms' climate exposure factor (CEF) and its interaction with disaster indicators, controlling for firms' financials. Panel A uses firms' annualized excess returns as the dependent variable. Panel B uses change in investor climate aversion as the dependent variable, constructed in a two-step procedure following Gibson Brandon, Krueger, and Mitali (2021) based on quarterly 13-F holdings. Panel C uses return on assets (ROA) as the dependent variable. Unrealized refers to selected firms in Table 3, with zero realized climate damages throughout the sample period from September 2003 to March 2024. Realized refers to the remaining firms in Table 2. Disaster is a dummy variable that indicates the occurrence of a billion-dollar flood event from the NOAA database. Affected is a dummy variable that indicates whether the majority of firms' assets are in affected states. Control variables are explained in Table 2. We also control for industry and year/month fixed effects. Observations are the total number of firm-months. All variables except climate aversion are winsorized at the 1st and 99th percentiles. Investor climate aversion is winsorized at the 3rd and 97th percentiles. All explanatory variables are cross-sectionally normalized to zero mean and unit standard deviation. Robust *t*-statistics are in parentheses, with standard errors estimated using Newey-West correction for 12 lags. ***1% significance; **5% significance; *10% significance.

Panel A: Stock Returns						
	Unrealized				Realized	
	(1) $E[R_{i,t}]$-RF	(2) $E[R_{i,t+1}]$-RF	(3) $E[R_{i,t+2}]$-RF	(4) $E[R_{i,t+6}]$-RF	(5) $E[R_{i,t}]$-RF	(6) $E[R_{i,t+6}]$-RF
CEF_i	1.91***	2.26***	0.78**	0.81**	−1.74***	−0.57
	(5.92)	(7.02)	(2.44)	(2.49)	(−3.94)	(−1.27)
$Disaster_t$	16.84***	−2.45**	−28.34***	8.47***	14.93***	11.92***
	(17.38)	(−2.53)	(−29.38)	(8.57)	(10.30)	(8.07)
$CEF_i \times Disaster_t$	−1.17***	−1.83***	2.37***	2.24***	1.43***	−1.45***
	(−3.39)	(−5.30)	(6.90)	(6.41)	(2.59)	(−2.59)
$CEF_i \times Disaster_t \times Affected_{i,t}$	−0.56**	0.09	−0.34	−0.25	−0.26	−1.58***
	(−2.08)	(0.33)	(−0.20)	(−0.91)	(−0.65)	(−3.90)
Controls	Yes	Yes	Yes	Yes	Yes	Yes
Industry FE	Yes	Yes	Yes	Yes	Yes	Yes
Year/Month FE	Yes	Yes	Yes	Yes	Yes	Yes
Cluster SE by Firm	Yes	Yes	Yes	Yes	Yes	Yes
Cluster SE by Year/Month	Yes	Yes	Yes	Yes	Yes	Yes
Observations	417,529	418,934	416,000	404,787	218,428	211,823

Table 7
(Continued)

	Panel B: Investor Climate Aversion				Panel C: Profitability	
	Unrealized				Unrealized	Realized
	(1) $\Delta ICA_{i,t} \times 10^4$	(2) $\Delta ICA_{i,t+1} \times 10^4$	(3) $\Delta ICA_{i,t+2} \times 10^4$	(4) $\Delta ICA_{i,t+6} \times 10^4$	(5) $ROA_{i,t+6} \times 10^2$	(6) $ROA_{i,t+6} \times 10^2$
CEF_i	1.51***	1.45***	0.84**	1.06***	0.60***	−1.18***
	(3.76)	(3.60)	(2.08)	(2.61)	(9.32)	(−14.22)
$Disaster_t$	19.23***	6.28***	−4.50***	8.27***	−0.64	0.26
	(15.06)	(5.24)	(−3.54)	(6.43)	(−3.23)	(0.93)
$CEF_i \times Disaster_t$	−1.72***	−1.28***	−0.03	0.46	0.25***	0.10
	(−3.81)	(−2.83)	(−0.07)	(1.02)	(3.52)	(0.93)
$CEF_i \times Disaster_t \times Affected_{i,t}$	0.45	0.06	0.07	0.20	−0.02	−0.77***
	(1.34)	(0.18)	(0.21)	(0.59)	(−0.31)	(−10.22)
Controls	Yes	Yes	Yes	Yes	Yes	Yes
Industry FE	Yes	Yes	Yes	Yes	Yes	Yes
Year/Month FE	Yes	Yes	Yes	Yes	Yes	Yes
Cluster SE by Firm	Yes	Yes	Yes	Yes	Yes	Yes
Cluster SE by Year/Month	Yes	Yes	Yes	Yes	Yes	Yes
Observations	331,108	332,138	331,315	327,238	378,614	197,061

Table A1
Physical Asset Climate Vulnerability

This table reports the summary statistics for the calibration of asset-level flood damage functions. Panel A summarizes the calibrated vulnerability parameter κ and goodness-of-fit measured by R^2. R^2 is calculated based on the squared deviations of model-implied damage factors and observed damage factors from the JRC database, although our subsequent jump-diffusion setup requires a damage curve that passes the origin. N is the number of scatters used to fit the damage curve. A graphical representation of these damage curves is shown in Figure 2. Panel B presents the overall goodness-of-fit of alternative damage functional forms including shifted sigmoid, hyperbolic tangent, arctangent, and hill functions. The overall R^2 is calculated as the R^2 of each asset type weighted by its asset count in the United States recorded in S&P Trucost dataset and aggregated together.

Panel A: Exponential CDF Damage Curves			
Asset Type	N	κ	R^2
Residential Building	9	0.848	0.894
Commercial Building	9	0.430	0.986
Industrial Building	9	0.699	0.997
Transport	9	0.817	0.990
Infrastructure Road	9	0.538	0.993
Agriculture	9	0.539	0.986
Panel B: Exponential CDF Damage Curves			
Damage Function	Expression		R^2
Exponential CDF	$h(x) = 1 - \exp(-\kappa x)$		
Overall			0.985
Shifted Sigmoid	$h(x) = \frac{2}{1+\exp(-kx)} - 1$		
Overall			0.972
Hyperbolic Tangent	$h(x) = \tanh(kx)$		
Overall			0.972
Arctangent	$h(x) = \frac{2}{\pi}\arctan(kx)$		
Overall			0.950
Hill	$h(x) = \frac{x}{k+\lvert x\rvert}$		
Overall			0.907

Table A2
Asset Damage Distribution Calibration

This table documents the summary statistics for asset-level log fractional damages J due to flood events under the business-as-usual (RCP8.5) climate scenario. To provide a snapshot of the future climate impact, we report the calibrated damage distributions for a (location-wise) median and top 5% most intense US flood event in 2030, 2050 and 2080 across the columns. Panel A shows results for coastal floods, while Panel B shows results for riverine floods. For each panel, μ_G, β_G and κ are parameters of $Gumbel(\kappa\mu_G, \kappa\beta_G)$ distribution from which we generate a sample of N log damages. We report estimated parameters for a Merton jump and a hybrid normal-exponential jump respectively. For the hybrid distribution, we set a tail probability $p = 0.3$ and calculate the corresponding climate value-at-risk J_p. The negative location parameter values are due to the negative imaginary part of the calibrated distributions, which we ceil at zero subsequently. We report the theoretical Cramér-von Mises criterion W^2, implemented with Simpson integration (excluding the negative part), which measures the aggregate squared deviations of Merton/hybrid from the original Gumbel distribution. Plots of the density curve for the median coastal and riverine floods are shown in Figure 3 and Figure 4 respectively.

	Median Expected Climate Damage			Top 5% Expected Climate Damage		
	2030	2050	2080	2030	2050	2080
	(1)	(2)	(3)	(4)	(5)	(6)
Panel A: Coastal Flood						
Empirical Simulation						
Gumbel μ_G	0.122	0.220	0.382	2.544	2.623	2.758
Gumbel β_G	0.029	0.019	0.074	0.077	0.053	0.171
Asset Vulnerability κ	0.699	0.699	0.699	0.699	0.699	0.699
N	10,000	10,000	10,000	10,000	10,000	10,000
Merton Jump Calibration						
Normal μ_N	0.097	0.162	0.297	1.809	1.855	1.996
Normal σ_N	0.026	0.017	0.066	0.068	0.048	0.152
Cramér-von Mises Distance W^2	1.687	1.092	4.312	4.445	3.101	9.903
Hybrid Jump Calibration						
Normal Core μ_N	0.089	0.156	0.277	1.788	1.841	1.950
Normal Core σ_N	0.017	0.011	0.044	0.045	0.031	0.100
Exponential Tail η	41.862	64.677	16.371	15.883	22.772	7.129
Tail Probability p	0.3	0.3	0.3	0.3	0.3	0.3
p Climate VaR J_p	0.106	0.167	0.320	1.833	1.872	2.050
Cramér-von Mises Distance W^2	0.151	0.098	0.317	0.398	0.278	0.863
Panel B: Riverine Flood						
Empirical Simulation						
Gumbel μ_G	-0.040	-0.001	-0.015	0.006	0.059	0.095
Gumbel β_G	0.112	0.007	0.048	0.341	0.247	0.323
Asset Vulnerability κ	0.699	0.699	0.699	0.699	0.699	0.699
N	10,000	10,000	10,000	10,000	10,000	10,000
Merton Jump Calibration						
Normal μ_N	0.017	0.002	0.008	0.141	0.140	0.196
Normal σ_N	0.100	0.006	0.042	0.305	0.220	0.288
Cramér-von Mises Distance W^2	3.851	0.274	1.686	14.368	10.717	14.073
Hybrid Jump Calibration						
Normal Core μ_N	-0.013	0.000	-0.004	0.050	0.074	0.109
Normal Core σ_N	0.066	0.004	0.028	0.201	0.145	0.190
Exponential Tail η	10.886	174.273	25.599	3.562	4.934	3.765
Tail Probability p	0.3	0.3	0.3	0.3	0.3	0.3
p Climate VaR J_p	0.052	0.004	0.023	0.249	0.218	0.298
Cramér-von Mises Distance W^2	0.093	0.011	0.053	0.638	0.820	1.054

Table A3
Firm Climate Exposure Summary by Industry

This table reports the top 10 industries by average firm climate exposure. The firm-level climate exposure measure is constructed based on Eq. 12. Panel A ranks the industries based on climate exposure factor (CEF), and Panel B and Panel C rank the industries based on absolute measures CEV and CEMV respectively. The industry classification is based on GIC first 6-digit code, as detailed in Table A4. We report the number of firms and within-industry mean, median and standard deviation of firm climate exposure for each of the top 10 industries. The "Total" line summarizes these statistics for the entire sample. We exclude industries with N < 10 in this table.

Panel A: Climate Exposure Factor (CEF)					
GIC 6	Industry	N	Mean	Median	Std. Dev.
41	Biotechnology	493	0.095	0.003	0.167
61	Electric Utilities	28	0.090	0.029	0.180
1	Energy Equipment & Services	56	0.081	0.033	0.152
43	Life Sciences Tools & Services	57	0.062	0.026	0.103
38	Health Care Equipment & Supplies	179	0.060	0.005	0.149
40	Health Care Technology	41	0.059	0.010	0.138
3	Chemicals	79	0.055	0.023	0.108
5	Containers & Packaging	21	0.051	0.026	0.080
44	Banks	352	0.049	0.035	0.056
56	Diversified Telecommunication Services	22	0.050	0.029	0.085
Total		4,349	0.046	0.015	0.096
Panel B: Climate Exposure Value (CEV)					
GIC 6	Industry	N	Mean	Median	Std. Dev.
61	Electric Utilities	28	1,930	496	2,654
63	Multi-Utilities	14	1,253	549	2,133
56	Diversified Telecommunication Services	22	761	3	2,170
30	Broadline Retail	20	760	3	2,947
23	Automobiles	25	654	0	3,050
18	Passenger Airlines	21	602	0	1,527
36	Household Products	11	422	22	1,131
17	Air Freight & Logistics	13	396	1	1,035
32	Consumer Staples Distribution & Retail	32	381	19	1,021
57	Wireless Telecommunication Services	10	313	0	947
Total		4,349	83	0	577
Panel C: Climate Exposure Market Value (CEMV)					
GIC 6	Industry	N	Mean	Median	Std. Dev.
13	Machinery	127	49,117	8	552,454
30	Broadline Retail	20	7,070	15	30,330
36	Household Products	11	6,070	54	10,774
53	Technology Hardware, Storage & Peripherals	27	4,698	0	21,053
31	Specialty Retail	124	4,067	0	28,531
39	Health Care Providers & Services	115	3,913	1	32,780
61	Electric Utilities	28	2,897	728	4,283
43	Life Sciences Tools & Services	57	2,361	3	16,880
32	Consumer Staples Distribution & Retail	32	2,134	29	6,433
63	Multi-Utilities	14	1,759	786	2,703
Total		4,349	2,065	0	94,775

Table A4
Industry Representation by Number of Firms

GIC 6	Industry Name	Sector	No. of Firms
1	Energy Equipment & Services	Energy	56
2	Oil, Gas & Consumable Fuels	Energy	125
3	Chemicals	Materials	79
4	Construction Materials	Materials	8
5	Containers & Packaging	Materials	21
6	Metals & Mining	Materials	56
7	Paper & Forest Products	Materials	7
8	Aerospace & Defense	Industrials	53
9	Building Products	Industrials	42
10	Construction & Engineering	Industrials	37
11	Electrical Equipment	Industrials	76
12	Industrial Conglomerates	Industrials	6
13	Machinery	Industrials	127
14	Trading Companies & Distributors	Industrials	44
15	Commercial Services & Supplies	Industrials	74
16	Professional Services	Industrials	89
17	Air Freight & Logistics	Industrials	13
18	Passenger Airlines	Industrials	21
19	Marine Transportation	Industrials	9
20	Ground Transportation	Industrials	35
21	Transportation Infrastructure	Industrials	4
22	Automobile Components	Consumer Discretionary	40
23	Automobiles	Consumer Discretionary	25
24	Household Durables	Consumer Discretionary	60
25	Leisure Products	Consumer Discretionary	26
26	Textiles, Apparel & Luxury Goods	Consumer Discretionary	41
27	Hotels, Restaurants & Leisure	Consumer Discretionary	120
28	Diversified Consumer Services	Consumer Discretionary	43
29	Distributors	Consumer Discretionary	9
30	Broadline Retail	Consumer Discretionary	21
31	Specialty Retail	Consumer Discretionary	124
32	Consumer Staples Distribution & Retail	Consumer Staple	32
33	Beverages	Consumer Staple	21
34	Food Products	Consumer Staple	76
35	Tobacco	Consumer Staple	6
36	Household Products	Consumer Staple	11
37	Personal Care Products	Consumer Staple	37
38	Health Care Equipment & Supplies	Health Care	179
39	Health Care Providers & Services	Health Care	115
40	Health Care Technology	Health Care	41
41	Biotechnology	Health Care	493
42	Pharmaceuticals	Health Care	158
43	Life Sciences Tools & Services	Health Care	57
44	Banks	Financials	356
45	Financial Services	Financials	76
46	Consumer Finance	Financials	37
47	Capital Markets	Financials	91
48	Mortgage Real Estate Investment Trusts (REITs)	Financials	2
49	Insurance	Financials	106

Table A4
(Continued)

GIC 6	Industry Name	Sector	No. of Firms
50	IT Services	Information Technology	57
51	Software	Information Technology	268
52	Communications Equipment	Information Technology	54
53	Technology Hardware, Storage & Peripherals	Information Technology	27
54	Electronic Equipment, Instruments & Components	Information Technology	109
55	Semiconductors & Semiconductor Equipment	Information Technology	88
56	Diversified Telecommunication Services	Communication Services	22
57	Wireless Telecommunication Services	Communication Services	10
58	Media	Communication Services	70
59	Entertainment	Communication Services	50
60	Interactive Media & Services	Communication Services	53
61	Electric Utilities	Utilities	28
62	Gas Utilities	Utilities	11
63	Multi-Utilities	Utilities	14
64	Water Utilities	Utilities	12
65	Independent Power and Renewable Electricity Producers	Utilities	11
66	Diversified REITs	Real Estate	3
67	Industrial REITs	Real Estate	1
68	Hotel & Resort REITs	Real Estate	1
69	Office REITs	Real Estate	1
70	Health Care REITs	Real Estate	0
71	Residential REITs	Real Estate	1
72	Retail REITs	Real Estate	0
73	Specialized REITs	Real Estate	1
74	Real Estate Management & Development	Real Estate	43
Total			4349

Table A5
Correlation with Alternative Climate Exposure Measures

This table documents Pearson's correlation coefficients for our firm-level climate exposure measures based on asset ownership with selected alternative climate exposure measures. As defined in Eq. 12, CEF is the intensity-based measure, CEV is the book value of total expected climate damages, and CEMV is the market value of climate damages estimated by Tobin's Q. This table reports the correlations based on the realization of these measures under the business-as-usual (RCP8.5) scenario. N is the number of firms.

Measure	CEF	CEV	CEMV	N
Carbon				
GHG1	0.008	0.452	0.004	3,064
GHG2	-0.001	0.537	0.022	3,064
GHG3 Up	0.002	0.464	0.017	3,064
GHG3 Down	0.002	0.464	0.017	3,021
GHG1 Int	0.032	0.000	-0.005	3,048
GHG2 Int	0.000	-0.004	0.000	3,048
GHG3 Up Int	-0.004	-0.003	-0.001	3,048
GHG3 Down Int	-0.025	-0.002	-0.006	3,008
S&P Firm Climate Sensitivities				
Fluvial Flood Score	-0.082	0.146	0.001	3,525
Pluvial Flood Score	-0.079	0.149	0.001	3,367
Wildfire Score	-0.082	0.146	0.001	3,525
Drought Score	-0.082	0.059	0.001	3,522
Earnings Call (Sautner et al., 2023)				
Climate Reg	-0.003	0.077	-0.004	3,509
Climate Opp	-0.010	0.135	-0.003	3,509
Climate Phy	0.010	0.030	-0.002	3,509
Climate Tot	-0.008	0.141	-0.005	3,509

Table A6
Bivariate Portfolio Sorting

This table summarizes the performance of portfolios sequentially sorted on a financial characteristic and climate exposure factor (CEF). Panel A reports CEF–size (ME) bivariate sorting. Panel B reports CEF–value (B/M) bivariate sorting. Panel C reports CEF–profitability (ROE) bivariate sorting. We divide the firms by a financial characteristic (size, value, or profitability) first into tercile groups and, within each group, we form quintile-sorted portfolios based on CEF. The portfolios are annually rebalanced based on March characteristics, with median returns and *t*-stats shown in the table. Returns (in %) are annualized by multiplying the monthly returns by 12. Robust *t*-statistics are in parentheses, with standard errors estimated using Newey-West correction for 12 lags. The sample period is September 2003 to March 2024.

Panel A: CEF × Size						
	(Low)				(High)	
ME Tercile	1	2	3	4	5	H-L
1 (Low)	−15.18	−15.35	−11.25	−1.62	−0.17	15.00
	(−2.70)	(−2.77)	(−2.18)	(−0.36)	(−0.03)	(6.00)
2	−2.54	2.18	7.03	8.21	8.32	10.86
	(−0.61)	(0.52)	(1.70)	(2.09)	(2.21)	(6.43)
3 (High)	6.99	9.15	9.19	10.27	9.78	2.79
	(1.89)	(2.57)	(2.57)	(2.93)	(2.80)	(2.18)
Panel B: CEF × Value						
	(Low)				(High)	
B/M Tercile	1	2	3	4	5	H-L
1 (Low)	−13.40	−5.61	4.23	8.83	10.77	24.18
	(−2.85)	(−1.19)	(1.02)	(2.43)	(3.21)	(11.38)
2	−5.96	0.97	6.83	7.84	7.54	13.50
	(−1.22)	(0.24)	(1.84)	(2.19)	(2.11)	(5.64)
3 (High)	−3.38	−0.80	5.82	10.25	7.46	10.85
	(−0.65)	(−0.16)	(1.31)	(2.24)	(1.50)	(3.90)
Panel C: CEF × Profitability						
	(Low)				(High)	
ROE Tercile	1	2	3	4	5	H-L
1 (Low)	−14.98	−15.91	−10.97	−4.20	0.39	15.38
	(−2.68)	(−2.72)	(−1.94)	(−0.74)	(0.07)	(9.87)
2	2.30	5.82	8.58	8.82	8.25	5.95
	(0.64)	(1.62)	(2.27)	(2.62)	(2.23)	(4.84)
3 (High)	2.93	8.16	9.67	9.18	10.42	7.49
	(0.71)	(2.08)	(2.67)	(2.48)	(2.89)	(5.39)

Table A7
Comparison of Matched and Dropped Firm Characteristics

This table reports summary statistics of matched and dropped firm characteristics between June 1999 and March 2024. Matched firms refer to the firms with at least 1 physical asset holding collected by the Trucost physical risk dataset, and dropped firms refer to the remaining firms (including delisted and ceased firms) from the JKP23 dataset. Log ME, B/M, ROE, I/A, K/A, S/A, and Lev are described in Table 2. Beta is the CAPM beta estimated in a 5-year rolling window. ΔS/S and ΔK/K are the annual growth rate of sales and physical assets respectively. GHG1/S and GHG2/S are carbon intensities, calculated as scope 1 and scope 2 GHG emissions respectively scaled by sales. GHG emissions respectively. E[R]–RF is the percentage monthly excess return, annualized by multiplying 12. N is the number of firm-months. We document summary statistics including pooled median, standard deviation, and the number of firm-months (subject to duplicate financial sin each quarter. All financial variables are winsorized at the 1st and 99th percentiles, and carbon intensities are winsorized at the 5th and 95th percentiles, to exclude extreme outliers.

	Matched Firms			Dropped Firms		
	Median	Std. Dev.	N	Median	Std. Dev.	N
Log ME	6.51	2.29	743,277	4.42	2.28	9,940,190
B/M	0.51	0.96	687,938	0.74	1.42	8,502,110
ROE	0.21	0.72	666,522	0.16	0.40	8,157,139
I/A	0.02	0.05	703,449	0.03	0.07	7,066,608
K/A	0.12	0.23	702,709	0.22	0.24	8,043,081
S/A	0.62	0.75	720,062	0.62	0.72	8,711,435
Lev	0.18	0.24	722,842	0.18	0.22	8,571,835
Beta	1.05	0.72	606,896	0.98	0.56	7,408,102
ΔS/S	0.07	0.74	682,887	0.06	0.92	8,095,689
ΔK/A	0.02	0.08	616,052	0.01	0.13	7,565,482
GHG1/S	11.48	332.82	317,228	21.02	603.55	34,227
GHG2/S	13.47	27.26	317,228	17.74	71.40	34,227
E[R]-RF	0.30	17.78	718,466	−0.42	18.83	9,549,348

Table A8
Pairwise Characteristics Matching

This table reports time-series average returns of a pairwise characteristics matching portfolio between September 2003 and March 2024. We calculate the return spread between the high-exposure firm and the low-exposure firm, $E[R_{Exp}–R_{Ins}]$, matched by the most recent characteristics in March. We match the firms by minimizing characteristic distance via Mahalanobis. We select the upper 50% pairs by CEF spread between the high-exposure and the low-exposure firms to increase the variation. Characteristics follow the setup in Table 5. The investor climate aversion (ICA) is constructed in a two-step procedure following Gibson Brandon, Krueger, and Mitali (2021). Return spread (in %) $E[R_{Exp}–R_{Ins}]$ is annualized by multiplying 12. Observations are the number of firm-months. Robust *t*-statistics are in parentheses, with standard errors estimated using Newey-West correction for 12 lags. ***1% significance; **5% significance; *10% significance.

	(1)	(2)	(3)	(4)	(5)	(6)	(7)
$E[R_{Exp,t+1}-R_{Ins,t+1}]$	2.60***	3.02***	3.01**	2.36***	3.77***	4.15***	3.45***
	(4.08)	(3.18)	(2.03)	(3.06)	(2.83)	(2.83)	(3.04)
Log $ME_{i,t}$	Yes	Yes	No	No	No	No	No
Log $B/M_{i,t}$	Yes	No	Yes	No	No	No	No
$ROE_{i,t}$	Yes	No	No	Yes	No	No	No
$I/A_{i,t}$	Yes	No	No	No	Yes	No	No
$K/A_{i,t}$	Yes	No	No	No	No	Yes	No
$S/A_{i,t}$	Yes	No	No	No	No	No	Yes
Distance	Mahalanobis	Mahalanobis	Mahalanobis	Mahalanobis	Mahalanobis	Mahalanobis	Mahalanobis
Observations	98,044	107,018	104,712	103,251	105,393	106,363	106,447

Table A9
Idiosyncratic Volatility Regressions

This table reports the time-series average of Fama-MacBeth regressions of stock excess returns against firms' climate exposure factor (CEF), idiosyncratic volatility (IVOL), their interaction (CEF × IVOL), and other financial characteristics. Column (1) and (2) present regression results without and with industry fixed effects based on the GIC 4-digit classification. All variables are winsorized at the 1st and 99th percentiles to account for extreme outliers. All explanatory variables are cross-sectionally normalized to zero mean and unit standard deviation. Observations are the number of firm-months. Robust *t*-statistics are in parentheses, with standard errors estimated using Newey-West correction for 12 lags. ***1% significance; **5% significance; *10% significance.

	(1)	(2)
CEF	−0.70	−0.46
	(−1.00)	(−0.75)
IVOL	−5.21***	−5.34***
	(−3.77)	(−3.97)
CEF × IVOL	2.23***	1.96***
	(2.66)	(2.62)
Log ME	−0.88**	−0.83
	(−0.63)	(−0.59)
Log B/M	1.61	2.07**
	(1.43)	(2.14)
ROE	1.01	0.93*
	(1.64)	(1.70)
I/A	0.27	0.11
	(0.31)	(0.22)
Industry FE	No	Yes
Model	FM	FM
Adj R^2	0.03	0.08
Observations	450,667	450,667

Table A10
Billion-Dollar Flood Events

This table summarizes (CPI-adjusted) billion-dollar flood events occurred in the US between 1999 and 2024 documented in the NOAA database.

No.	Flood Event	Months	Affected States
1	South Florida Flooding	Oct 2000	FL
2	Northeast Flooding	Jun 2006	NY/PA/DE/MD/NJ/VA
3	Midwest Flooding	Jun 2008	IA/IL/IN/MO/MN/NE
4	Georgia Flooding	Sep 2009	GA
5	Northeast Flooding	Mar 2010	RI/CT/MA/NJ/NY/PA
6	East/South Flooding and Severe Weather	May 2010	TN/AR/KY/GA
7	Mississippi River Flooding	Apr - May 2011	AR/TN/MS/MO/LA
8	Missouri River Flooding	May - Jun 2011	MT/ND/SD/NE/IA/KS/MO
9	Illinois Flooding and Severe Weather	Apr 2013	IL/IN/MO
10	Colorado Flooding	Sep 2013	CO
11	Michigan and Northeast Flooding	Aug 2014	MI/MD/NY
12	Texas and Oklahoma Flooding and Severe Weather	May 2015	TX/OK
13	South Carolina and East Coast Flooding	Oct 2015	SC/GA
14	Texas and Louisiana Flooding	Mar 2016	TX/LA
15	Houston Flooding	Apr 2016	TX
16	West Virginia Flooding and Ohio Valley Tornadoes	Jun 2016	WV/OH
17	Louisiana Flooding	Aug 2016	LA
18	California Flooding	Feb 2017	CA
19	Missouri and Arkansas Flooding and Central Severe Weather	Apr - May 2017	MO/AK/IL
20	Missouri River and North Central Flooding	May 2019	NE/IA/MO/SD/MN/ND/WI/MI
21	Arkansas River Flooding	May - Jun 2019	OK/AK
22	Mississippi River, Midwest and Southern Flooding	Mar - Jul 2019	OK/NE/MO/IL/KS/AK/KY/TN/TX/MS/LA
23	California Flooding and Severe Weather	Jan 2021	CA
24	Louisiana Flooding	May 2021	LA
25	Kentucky and Missouri Flooding	Jul 2022	KY/MO
26	California Flooding	Dec 2022 - Mar 2023	CA
27	Fort Lauderdale Flash Flood	Apr 2023	FL
28	Northeastern Flooding and North Central Severe Weather	Jul 2023	VT/NY
29	East Coast Storm and Flooding	Dec 2023	SC/NJ/NY/CT
30	Upper Midwest Flooding	Jun 2024	MN/SD/IA/WI/MI